frontiers | Frontiers in Energy Research

TYPE Review
PUBLISHED 07 March 2023
DOI 10.3389/fenrg.2023.1135093

OPEN ACCESS

EDITED BY
Uwe Schröder,
University of Greifswald, Germany

REVIEWED BY
Muslum Demir,
Osmaniye Korkut Ata University, Türkiye
Mingjiang Xie,
Huanggang Normal University, China

*CORRESPONDENCE
Yang Haiping,
yanghaiping@hust.edu.cn

SPECIALTY SECTION
This article was submitted to Bioenergy and Biofuels, a section of the journal Frontiers in Energy Research

RECEIVED 31 December 2022
ACCEPTED 20 February 2023
PUBLISHED 07 March 2023

CITATION
Xiaorui L and Haiping Y (2023), A state-of-the-art review of N self-doped biochar development in supercapacitor applications. *Front. Energy Res.* 11:1135093. doi: 10.3389/fenrg.2023.1135093

A state-of-the-art review of N self-doped biochar development in supercapacitor applications

Liu Xiaorui[1] and Yang Haiping[2]*

[1]School of Mines, China University of Mining and Technology, Xuzhou, China, [2]State Key Laboratory of Coal Combustion, School of Energy and Power Engineering, Huazhong University of Science and Technology, Wuhan, China

Due to its renewability, eco-friendliness, and cost-effectiveness, biochar is a promising alternative to fossil fuel-based carbon for electrode material application in supercapacitors. However, pristine biochar often exhibits poor structure and low activity, which strongly inhibit its commercial utilization. N-doping is an efficient way to improve the electrochemical performance of biochar by enhancing the conductivity and surface wettability that further induce a pseudo-capacitance effect. Compared with external doping, the synthesis of N self-doped biochar from natural N-rich biomass without using external N precursors, which are harmful and costly, has attracted increasing attention. Few reviews of N-doped biochar applications in supercapacitors are available, and studies of N self-doped biochar are still scarce. This paper reviews the developments over the past 10 years on the preparation, activation, and application of N self-doped biochar in supercapacitors. Notably, the evolution of N-functionalities during N self-doped biochar production with or without activating agents was analyzed. The relationships between N content and the specific capacitance and the contribution of N self-doping-induced pseudo-capacitance to the total specific capacitance are also discussed. Finally, the challenges and the prospects of N self-doped biochar applications in supercapacitors are proposed.

KEYWORDS

biomass, N self-doped biochar, N functionality, electrochemical performance, supercapacitor

1 Introduction

The excessive consumption of fossil fuels (coal, gas, and oil) gives rise to energy crisis, environmental pollution, and global warming (Parsimehr et al., 2022; Zhang et al., 2022). According to a statistical report (IPCC, 2022), the average annual emission levels of the last decade (2010–2019) were higher than in any previous decade for each group of greenhouse gases (GHGs). Compared to 1990, CO_2, CH_4, and N_2O from fossil fuel and industry in 2019 grew by 67%, 29%, and 33%, respectively. Due to this, renewable energy, such as solar energy, wind energy, and hydropower, developed rapidly in the past decades. However, in comparison to fossil fuels, these renewable energies have the main disadvantage of intermittency (Li et al., 2021) because they fluctuate with seasons, circadian cycles, and weather, leading to the fluctuation of generating capacity. Therefore, to ensure the security of the power grid, energy storage facilities are required when using solar and wind energy for power generation.

Supercapacitors are a promising energy storage technique because of their high power density, rapid charging/discharging rate, long cycle life, excellent reversibility, *etc.* (Yan et al., 2014). However, lower energy density greatly limits their large-scale utilization. The electrode material is the critical factor affecting the energy density of supercapacitors (Bo et al., 2019; Huang et al., 2019). Thus, improving the electrochemical properties of electrode materials is the most convenient and effective way to increase energy density. To date, carbon-based materials, such as graphene, activated carbon, carbon nanotube, and carbon aerogel, are widely used as electrode materials in supercapacitors because of their high conductivity, large surface area, tunable porosity, superior stability, and enriched electroactive sites (Zhu and Xu, 2020; Wesley et al., 2022). However, these carbon materials are mainly derived from fossil materials using complex and costly procedures that are greatly harmful to the environment and human health (Zhu and Xu, 2020). Thus, there is an urgent need to explore an eco-friendly, sustainable, and cost-efficient resource for carbon material production.

As the only carbon-based renewable energy resource, biomass is considered an alternative to fossil fuels because it can not only be used for power generation and heat supply but can also be converted into syngas, bio-oil, and biochar products by thermochemical and biochemical techniques. Because biomass is derived from the photosynthetic process of CO_2 and H_2O in nature, almost zero or even negative CO_2 emissions can be achieved during its cycle life. Due to the renewability, abundance, and accessibility of biomass feedstock, biochar is considered an effective electrode material for supercapacitors (Liang et al., 2018; Cuong et al., 2021). There are also other advantages for biochar application as electrode material, such as its physical and chemical stability, large surface area, and developed porous structure, which are beneficial to ion transport (Tang et al., 2017), the abundant surface functional groups (e.g., N-, O-, S-, and P-containing functional groups), and the ability to deal with solid waste in large quantities (Cuong et al., 2021). Moreover, biochar is low cost because it is often the main product from biomass or a by-product when biomass is used to produce bio-oil or syngas (Zhu and Xu, 2020). Meyer et al. also reported that the cost of biochar production is far less than that of activated carbon and graphitic carbon (Meyer et al., 2011).

Various techniques have been developed for biochar production, such as pyrolysis, hydrothermal carbonation, torrefaction, and microwave-assisted pyrolysis. However, biochar in its raw form often exhibits poor porous structure and low activity that is adverse to its utilization in supercapacitors (Cuong et al., 2021). To further improve the electrochemical performance, modification of biochar is essential. To date, two methods are commonly used: 1) activation by physical and chemical activators to defuse the porous structure of biochar (Hu et al., 2022). The physical activators refer to CO_2, H_2O, and air, while the frequently used chemical activators include KOH (Qin et al., 2022), H_3PO_4 (Li et al., 2022), and $ZnCl_2$ (Lima et al., 2022); 2) doping of heteroatoms such as N, P, and S to enrich surface functional groups (Li et al., 2022; Xia et al., 2022). Among these heteroatoms, N-doping is most implemented due to easily available and low-cost N sources such as NH_3, urea, and melamine (Bai et al., 2021; Mehdi et al., 2022; Yuan et al., 2022). Doping of N heteroatoms can enhance conductivity and surface wettability, and induce a pseudo-capacitance effect of the carbon material, thereby improving its energy/power density with versatile properties (Gopalakrishnan and Badhulika, 2020). Thus, the specific capacitance of N-doped biochar is the sum of the electrical double-layer capacitance and the pseudo-capacitance, significantly improving the performance of supercapacitors. More importantly, doping of N atoms can reduce lattice mismatching and increase electronic conductivity because N is the neighboring element of carbon in the periodic table (Gopalakrishnan and Badhulika, 2020). Usually, to achieve a better modification effect, these two methods are often implemented in combination with each other.

All kinds of biomass can be employed as the feedstock for biochar production, including agricultural waste (Lang et al., 2021; Jiang et al., 2022), tea waste (Wesley et al., 2022), woody biomass (Ma et al., 2021; Chen et al., 2022), seeds (Liang et al., 2021), animal waste (Qin et al., 2022; Wang et al., 2022), fungal waste (Li et al., 2021), vegetables (Li et al., 2022; Xue et al., 2022), and starch (Li et al., 2020; Yuan et al., 2021. Among the various types of biomass, it is worth noting that some naturally have a higher N content, for example, algae (Yuan et al., 2022), mushrooms (Xue et al., 2022), spent coffee ground (Sangprasert et al., 2022), bean pulp (Ding et al., 2021), pharmaceutical drug residues (Zhang et al., 2021; Chen et al., 2022), amino acids (Guo et al., 2021), *etc.* The bio-oil and syngas production from these N-rich biomasses usually contain high levels of N-containing components, leading to the molecular oligomerization, viscosity, and emission of NOx during subsequent combustion (Jiang et al., 2022). Therefore, N self-doped biochar is a preferentially expected product for N-rich biomass utilization. Compared with the co-pyrolysis of biomass and extra N precursors, the self-doping strategy *via* pyrolyzing N-rich biomass is eco-friendly and cost-effective because the use of extra N sources is avoided (Wang et al., 2020; Liu et al., 2022). By comparing the environmental performance of a biochar aerogel-based electrode (BA-electrode) and a graphene oxide aerogel-based electrode (GOA-electrode) using the life cycle assessment method, Jiang et al. (2021) found that the life cycle global warming potential for the BA electrode was lower than that of GOA electrode, with a reduction of 53.1–68.1%. Compared to a GOA electrode, the environmental damages of a BA electrode were greatly decreased by 35.8–56.4%, 44.9–62.6%, and 87.0–91.2% for human health, ecosystems, and resources, respectively. Due to these advantages, producing N self-doped biochar using N-rich biomass feedstocks is attracting increasing attention. Various strategies for N self-doped biochar production have been reported. Understanding the existing strategies and the performance of supercapacitors using N self-doped biochar as the electrode material is of great significance to future research. In this study, the latest developments in the preparation, activation, and application of N self-doped biochar in supercapacitors are reviewed. Notably, the evolution of N-functionalities during N self-doped biochar production with or without activating agents and the impact of N self-doping on the electrochemical performance are discussed. Although numerous reports with respect to biochar utilization in supercapacitors are available, reviews on N self-doped biochar for supercapacitor application are still scarce.

2 Preparation of N self-doped biochar

The preparation of N self-doped biochar usually involves some or all of the following steps: 1) pretreatment of the raw biomass, 2) pre-carbonization or pre-activation in mild conditions, 3) pyrolysis/

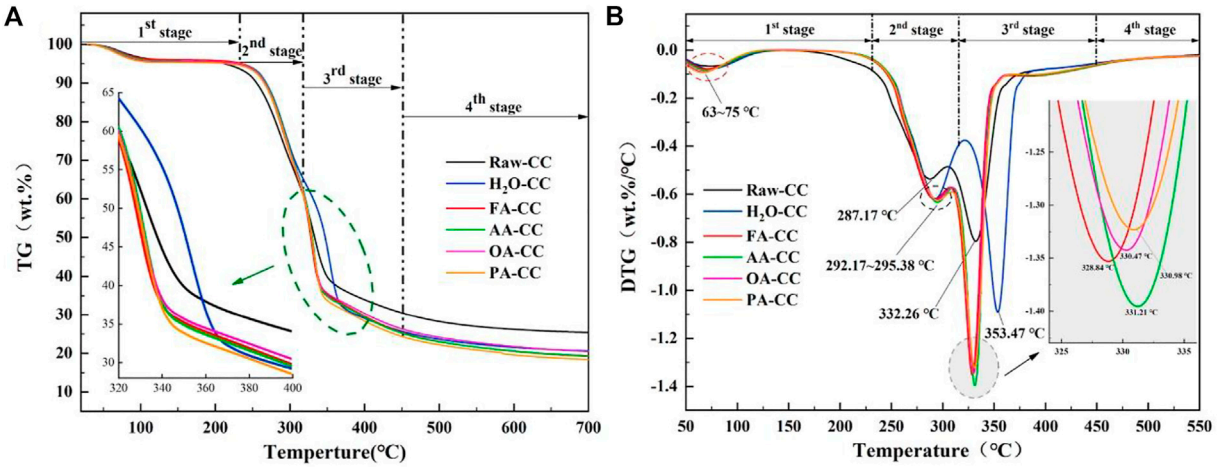

FIGURE 1
(A) Thermogravity (TG) and **(B)** differential thermogravimetry (DTG) curves for raw and washing pretreated samples (Liu et al., 2022).

carbonization or activation with one or more step(s), 4) post-treatment of the solid product. Because the activation is often implemented simultaneously with pre-carbonization or pyrolysis, the activation is introduced together with the preparation procedures in this review.

2.1 Pretreatment methods

The inorganic elements naturally occurring in biomass are considered to be unfavorable to the electrochemical performance of biochar. Zhu et al. reported that excessive residual metal content in algal biomass plays the role of "dead mass," resulting in a less-developed porous structure (Zhu et al., 2018). Therefore, raw material is often pretreated to remove the impurities before carbonization. Washing with acetone (Fu et al., 2018), ethanol (Yan, 2020), deionized water (Sinha et al., 2020), distilled water (Yan et al., 2020), or ultrapure water (Liu et al., 2017) or washing/soaking in acid solutions such as HCl (Wen et al., 2019), H_2SO_4 (Sattayarut et al., 2019), HNO_3, and acetic acid/H_2O_2/HF/$NaClO_2$ (Wang et al., 2019), or the combination of them, are most frequently performed. It was reported that washing with water (H_2O-CC), formic acid (FA-CC), acetic acid (AA-CC), oxalic acid (OA-CC), and propionic acid (PA-CC) showed significant effects on the pyrolysis characteristic of corn cob (CC) (Figure 1) (Liu et al., 2022). When acid washing is employed, water washing is required to remove the residual acids. Then, the washed biomass is dried in an oven at 60–110 °C or freeze-dried (Li et al., 2019; Zhu et al., 2019) to remove the extra moisture. The washed and dried biomass is cut into small pieces or ground into powders with the desired sizes manually in a mortar or by an automatic mill. However, the washing of biomass is still under debate because some researchers (Gao et al., 2021; Qin et al., 2022) have found that the presence of the inorganics in the raw biomass actually promoted the development of pores. This might be attributed to the diversity of biomass feedstock and types of inorganics. Thus, the impact of pretreatment on the performance of biochar is still unclear. It is necessary to clarify the effects of inorganics on the physiochemical properties of biochar so that the pretreatment of the feedstock can be rationally performed.

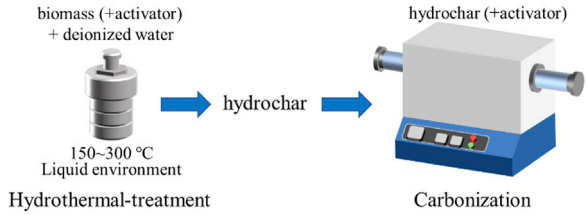

FIGURE 2
Typical procedure for hydrothermal treatment combined with pyrolysis.

2.2 Pre-carbonization/pre-activation

Hydrothermal carbonization is a mild thermochemical conversion process requiring a liquid environment under autogenous pressures (2–10 MPa) at 150–300°C. It is mainly explored to deal with wetland plants and biomass with high moisture content to produce bio-oil and hydrochar (Soroush et al., 2022). It consumes less energy than pyrolysis because it does not require a pretreatment step (MacDermid-Watts et al., 2020; Stobernack et al., 2020). Generally, the hydrochar exhibits low surface area and poor porous structure. For example, the hydrochar derived from cow manure obtained its largest surface area and pore volume of only 6.114 m^2/g and 0.021 cm^3/g, respectively (Liu et al., 2019). However, due to the high hydrochar yield of 40–70 wt% (Zhu and Xu, 2020), hydrothermal treatment is sometimes employed as a pre-carbonization or pre-activation strategy before pyrolysis to yield carbon precursors for N self-doped biochar production, as shown

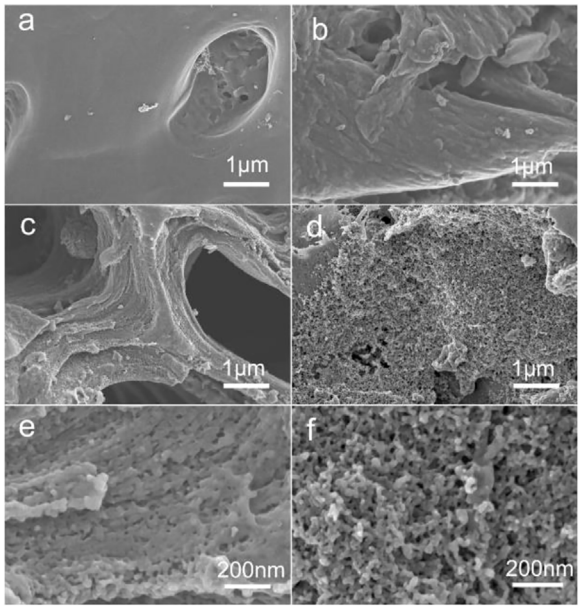

FIGURE 3
SEM images of peanut shell-derived biochar: **(A)** carbonized in molten Na_2CO_3–K_2CO_3 salt without hydrothermal pre-treatment, **(B)** hydrothermal pre-treatment for 12 h before carbonization, **(C, E)** hydrothermal pre-treatment for 24 h before carbonization, and **(D, F)** hydrothermal pre-treatment for 48 h before carbonization (Lei et al., 2021).

in Figure 2 (Si et al., 2013; Rong et al., 2019; Wen et al., 2019; Hu et al., 2022). A hydrothermal process also has the ability to insert or stabilize foreign atoms into the carbon matrix (Yu et al., 2021; Sangprasert et al., 2022) and etch pores to a certain extent due to the hydrolyzation of hemicellulose and cellulose (Lei et al., 2021; Hu et al., 2022). Thus, modification of functional groups and the porous structure can be achieved by changing the solvent medium (Rawat et al., 2022). The formation of a pore structure and carbon skeleton is more beneficial to subsequent carbonization/activation compared to the parent biomass (Lei et al., 2021). Figure 3 displays the comparison of the morphologies of the peanut shell-derived biochar products prepared by Na_2CO_3–K_2CO_3 activation with/without hydrothermal pre-treatment. The surface structure of biochar was significantly enhanced by hydrothermal pre-treatment.

2.3 Stepwise pyrolysis

Pyrolysis, which is performed in an oxygen-limited atmosphere at elevated temperatures, is a well-developed and widely used thermochemical conversion technique for biochar production due to its advantages of flexibility, speed, economy, eco-friendliness, and large capacity (Yuan et al., 2021). Pyrolysis is traditionally divided into slow, fast, and flash pyrolysis according to the temperature, residence time, and heating rate (Li et al., 2020; Zhou et al., 2021). Slow pyrolysis refers to the pyrolysis process performed at temperatures lower than 500 °C with a heating rate <10 °C/min and a residence time of several hours to days. Fast pyrolysis is often conducted at a temperature ranging from 500 °C to 900 °C, with a heating rate of 10–100 °C/min. The residence time assigned to fast pyrolysis is less than 10 s; however, it often varies from a few minutes to hours for biochar production. Flash pyrolysis, which is performed at a temperature of around 1,000 °C, with a heating rate >1,000 °C/min and a residence time <2 s, is explored, in particular for bio-oil production. For biochar preparation, slow pyrolysis is preferred due to the higher biochar yield of >30 wt%, followed by fast pyrolysis with a biochar yield of 10–12 wt%.

Considering the preparation of N self-doped biochar, one-step and two-step pyrolysis procedures are frequently used. During one-step pyrolysis (Figure 4), the pretreated biomass (Gao et al., 2015; Liu et al., 2017; He et al., 2019; Yu et al., 2019; Zhang et al., 2019; Sun et al., 2020) or the mixture of biomass and activating reagents (Chen et al., 2019; Lian et al., 2019; Zhao et al., 2020) is directly pyrolyzed in a furnace. For the two-step method, the pretreated biomass is first pre-carbonized and then activated with reagents (Figure 5A) (Zou et al., 2019; Biegun et al., 2020; Yan, 2020), carbonized after pre-activation (Figure 5B) (Wen et al., 2019), or successively pyrolyzed without an activator (Figure 5C) (Huang et al., 2018; Ma et al., 2019). Generally, the first step of the successive pyrolysis is also considered a pre-carbonization process (Wang and Liu, 2015). Pre-carbonization is reported to have the ability to remove impurities effectively and improve activation efficiency with reduced consumption of the activator (Jiao et al., 2022). In addition to these methods, a three-step strategy involving pre-carbonization, hydrothermal treatment, and activation was also implemented for N self-dope biochar production from walnut shells (Wang et al., 2018) and *Enteromorpha prolifera* (Ren et al., 2018).

Microwave-assisted pyrolysis is conducted using a microwave furnace with an electromagnetic spectrum frequency that ranges from 0.3 to 300 GHz and a wavelength that ranges from 1,000 to 1 mm (Sun et al., 2022). Microwave pyrolysis heats the samples uniformly based on the resonation of the microwave radiation frequency and that of water molecule vibration in the target samples. Therefore, microwave pyrolysis is typically appropriate to process biomass with a high moisture content. Microwave heating also has the advantages of energy efficiency and fast response (Zhang et al., 2022). A two-step pyrolysis procedure involving carbonization and microwave-assisted activation was employed by Foo and Hameed (2013) to prepare biochar from oil palm shells. As shown in Figure 6, the oil palm shell was first carbonized at 700 °C, and the produced char was then activated with KOH in a microwave oven.

Plasma is another effective technology to process material under mild conditions, with the advantages of being chemical-free and simple. For example, non-thermal plasma processing was applied to modify the biochar derived from bamboo shoot shells before it was used in contaminant removal and supercapacitor applications (Zhou et al., 2022). The biochar after plasma treatment exhibited enhanced hydrophilicity, larger surface area, and higher N/O content, leading to higher absorption capacity and the improvement of electrochemical performance.

Conventional pyrolysis, microwave-assisted pyrolysis, and plasma treatment are all effective techniques for N self-doped biochar preparation. Conventional pyrolysis in a heating

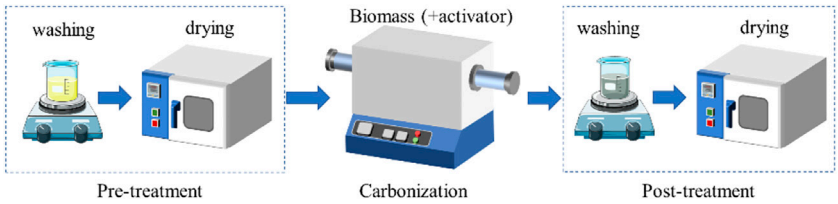

FIGURE 4
One-step method commonly used for N self-doped biochar production.

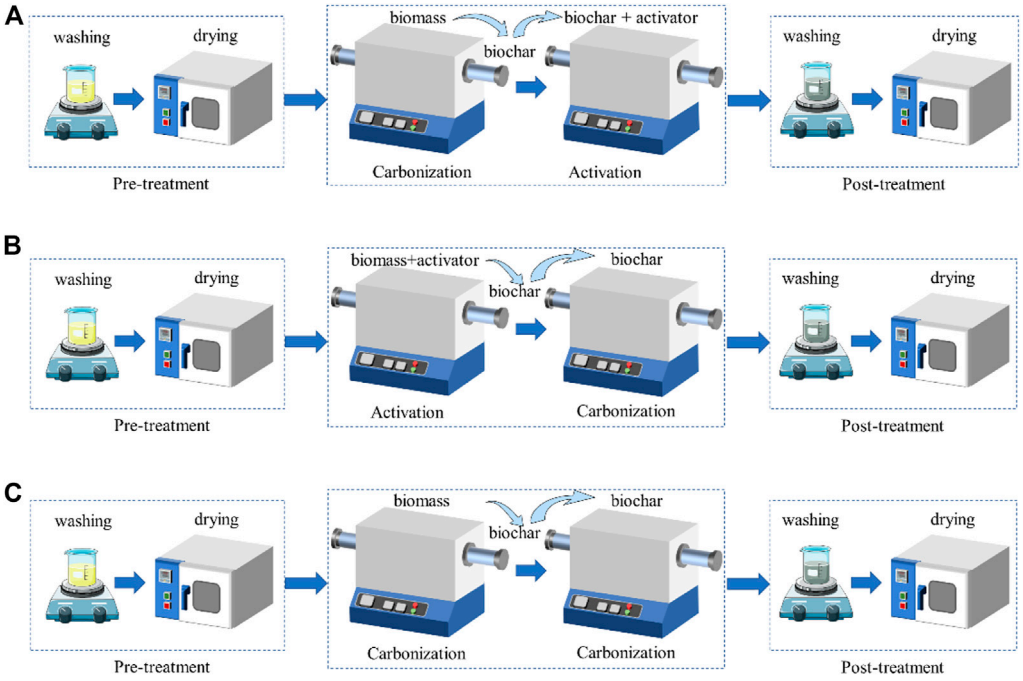

FIGURE 5
Two-step method commonly used for N self-doped biochar production. **(A)** pre-carbonization and activation, **(B)** pre-activation and carbonization, **(C)** successively pyrolysis.

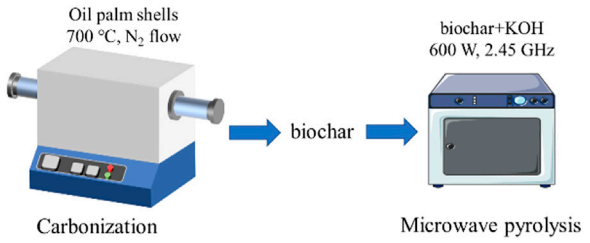

FIGURE 6
Two-step procedure of carbonization, followed by microwave activation.

furnace with a one-step or two-step strategy is still the mainstream method, while microwave-assisted and plasma pyrolysis are rarely reported.

2.4 Posttreatment

After these steps, the obtained N self-doped biochar is washed with dilute acid (HCl, H_2SO_4, HNO_3, *etc.*) solution to remove the inorganic impurities and subsequently washed by deionized/distilled/ultrapure water until neutral (Raj et al., 2018; Xu et al., 2018). Finally, the purified biochar is dried for further investigation of its electrochemical performance.

3 N self-doped biochar applications in supercapacitors

N self-doped biochar is produced from naturally N-rich biomass, including plants, animals, foods, algae, organic wastes, protein/amino acids, and fungus, as shown in Figure 7. Among these types, N-rich plant-based biomass is the most commonly used for N self-doped biochar production. Alkali hydroxides, especially KOH,

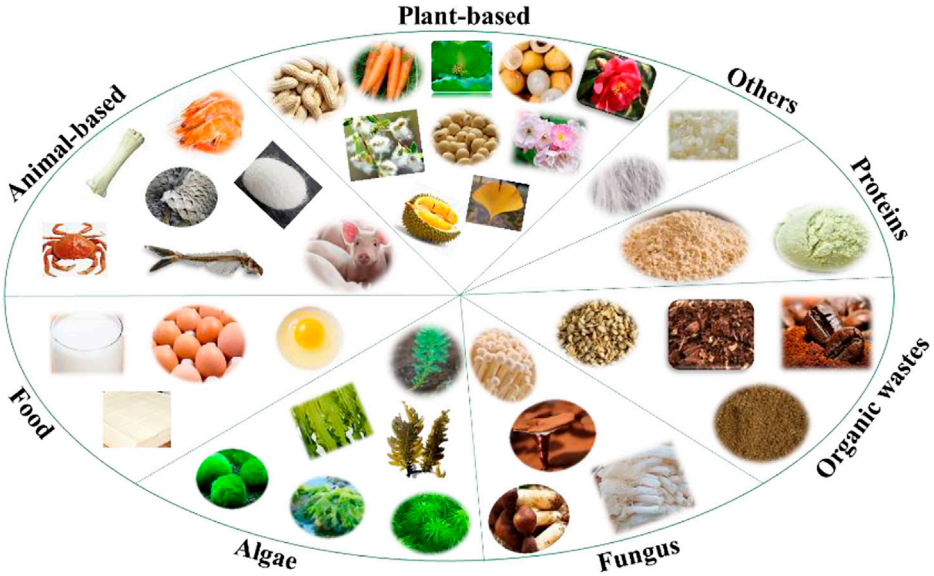

FIGURE 7
N-rich biomass involved in existing research.

are the favorite activating reagents due to their excellent pore etching ability, the mechanism of which is described as follows. First, KOH reacts with carbon to generate H_2 and CO_2 and simultaneously forms K_2CO_3 (R1). As the temperature reaches 700 °C, K_2CO_3 decomposes into K_2O and CO_2 (R2). Then, CO_2 reacts with carbon to form CO (R3). With the continuous increase of temperature, both K_2CO_3 and K_2O are reduced, accompanied by the release of CO and K vapor (R4 and R5). Finally, the gases and K vapor pass through the carbon matrix to activate the pore formation.

$$6KOH + 2C \rightarrow 2K + 3H_2 + 2\,K_2CO_3 \quad (R1)$$

$$K_2CO_3 \rightarrow K_2O + CO_2 \quad (R2)$$

$$CO_2 + C \rightarrow 2CO \quad (R3)$$

$$K_2CO_3 + 2C \rightarrow 2K + 3CO \quad (R4)$$

$$K_2O + C \rightarrow 2K + CO \quad (R5)$$

3.1 Plant-based N self-doped biochar

The N-rich plant-based biomass involves leaves, flowers, stems, barks, fruits, seeds, and roots of plants, as well as the derived straws that contain enriched protein or vitamins. For example, N-doping porous carbon fabricated from quinoa with KOH activation exhibited a special capacitance of 330 F/g at a density of 1 A/g (Sun et al., 2020). N, S co-doped hierarchical porous carbon was fabricated from ginkgo leaves *via* carbonization, followed by NaOH/KOH activation (Zhang et al., 2020). Due to the high specific surface area SSA (975 m^2/g) and higher heteroatom content (1.88% N and 1.87% S), the derived carbon exhibited a high specific capacitance of 333.4 F/g at 0.1 A/g. Jiao et al. reported a hierarchical porous biochar (1.7% N) from soybean straw produced by carbonization and mild activation with KOH (Jiao et al., 2022). The optimal sample exhibited a specific capacitance of 380.5 F/g at 0.5A/g. Protein-rich soybeans were also converted into a heteroatom self-doped biochar with KOH activation (Lin et al., 2018; Yan et al., 2020; Yu et al., 2021). Other plants used to prepare N self-doped biochar involving KOH activation for supercapacitor application include corn silk (Zhou et al., 2020), *Broussonetia papyrifera* stem bark (Wei et al., 2015), *Moringa oleifera* branches (Cai et al., 2016), walnut shells (Wang et al., 2018), longan shell (Yan, 2020), broad bean shells (Xu et al., 2015), longan pulp (Wang et al., 2020), lotus leaves (Liu et al., 2020), *Viburnum sargentii* leaves (Zhang et al., 2019), *Samanea saman* leaves (Sattayarut et al., 2019), willow catkins (Wang et al., 2015), tobacco rods (Zhao et al., 2016), fallen *Camellia* flowers (Guo et al., 2017), rose multiflora (Chen et al., 2018), pomelo peel (Fu et al., 2018), mung bean husk (Song et al., 2019), cotton seed husks (Chen et al., 2018), bamboo shoot shells (Han et al., 2018), metasequoia fruit (Jia et al., 2019), and soybean root (Guo et al., 2016), as shown in Table 1.

On account of the strong corrosivity of KOH, moderate activating reagents such as carbonates and chlorides are considered to be the alternatives. Foxtail grass seeds were carbonized at 550–750 °C with $NaHCO_3$/$KHCO_3$ to prepare a self-doped biochar (Liang et al., 2021). Benefiting from the large SSA of 819 m^2/g and a high N content of 2.52 at.%, the as-prepared biochar displayed a high gravimetric capacitance of 358.0 F/g at 0.5 A/g. N self-doped carbon materials were also prepared from eucalyptus leaves (Mondal et al., 2017) and fallen flowers of *Magnolia denudata* (Qi et al., 2018) with $KHCO_3$ activation. A heteroatom self-doped porous biochar (1.02 at% N) from peanut shells was prepared *via* hydrothermal carbonization, followed by Na_2CO_3–K_2CO_3 activation (Lei et al., 2021), showing a specific capacitance of 447 F/g at 0.2 A/g. Pine pollen was pyrolyzed with $MgCO_3$, and the derived carbon possessed a high specific capacitance of 419.6 F/g at 1A/g (Wan et al., 2019). Lily was

TABLE 1 Plant-based N self-doped biochar applications in supercapacitors.

Biomass	Pre-treatment	Preparation method	N content	*C*	*Es* (Wh/kg)	*Ws* (W/kg)	Ref
Quinoa	Ethanol/deionized water washing	Pre-carbonization followed by KOH activation	1.97%	330 F/g at 1 A/g	22	625	Sun et al. (2020)
Ginkgo leaves	Deionized water washing	Pre-carbonization followed by KOH/NaOH activation	1.88%	333.4 F/g at 0.1 A/g	–	–	Zhang et al. (2020)
Soybean straw	Deionized water washing	Pre-carbonization followed by KOH activation	1.7%	380.5 F/g at 0.5 A/g	8.95	25	Jiao et al. (2022)
Soybean	Deionized water washing	Pre-carbonization, hydrothermal treatment, and KOH activation	3.15 at %	685.1 F/g at 0.5 A/g	41.8	750	Yu et al. (2021)
Corn silk	–	Pre-carbonization followed by KOH activation	2.07%	291.2 F/g at 0.1 A/g	5.4	5,000	Zhou et al. (2020)
Broussonetia papyrifera stem bark	–	Hydrothermal treatment with KOH followed by carbonization	1.0 at %	320 F/g at 0.5 A/g	–	–	Wei et al. (2015)
Moringa oleifera branches	–	Impregnation with KOH followed by carbonization	1.3%	355 F/g at 0.5 A/g	20	178.6	Cai et al. (2016)
Walnut shells	–	Pre-carbonization, hydrothermal treatment with KOH followed by carbonization	0.89%	462 F/g at 1 A/g	42.8	1,249	Wang et al. (2018)
Broad bean shells	–	KOH activation	2.0%	202 F/g at 0.5 A/g	–	–	Xu et al. (2015)
Longan pulp	–	hydrothermal treatment, carbonization, and KOH/KCl activation	1.1%	380 F/g at 0.5 A/g	5.3	125.7	Wang et al. (2020)
Lotus leaves	Deionized water washing	Pre-carbonization followed by KOH activation	1.47 at %	523 F/g at 1 A/g	–	–	Liu et al. (2020)
Viburnum sargentii leaves	Ethanol/deionized water washing	Pre-carbonization followed by KOH activation	0.53 at %	612.8 F/g at 0.5 A/g	25.6	450	Zhang et al. (2019)
Samanea saman leaves	H_2SO_4/deionized water washing	KOH activation	4.6 at %	179 F/g at 0.5 A/g	78.5	829	Sattayarut et al. (2019)
Willow catkins	Deionized water washing	Impregnation with KOH followed by carbonization	2.51 wt%	340 F/g at 0.1 A/g	–	–	Wang et al. (2015)
Tobacco rods	–	Hydrothermal carbonization followed by KOH activation	1.23 wt%	286.6 F/g at 0.5 A/g	31.3	11,800	Zhao et al. (2016)
Rose multiflora	Deionized water washing	Pre-carbonization followed by KOH activation	1.2 at %	340 F/g at 0.5 A/g	52.6	700	Chen et al. (2018)
Pomelo peel	Acetone/deionized water washing	Pre-carbonization followed by KOH activation	4.47 at %	208.7 F/g at 1 A/g	7.25	260.8	Fu et al. (2018)
Mung bean husks	–	Pre-carbonization followed by KOH activation	0.73 at %	353 F/g at 1 A/g	20.4	872	Song et al. (2019)
Cotton seed husks	Deionized water washing	KOH activation	2.56 at %	238 F/g at 0.5 A/g	10.4	300	Chen et al. (2018)
Bamboo shoot shells	Ethanol/deionized water washing	KOH activation	1.9 wt%	223.21 F/g at 1 A/g	7.75	327.87	Han et al. (2018)
Metasequoia fruit	–	Pre-carbonization followed by KOH activation	2.42 at %	326 F/g at 0.5 A/g	7.6	129	Jia et al. (2019)
Soybean root	Ethanol/deionized water washing	Pre-carbonization followed by KOH activation	1.8 at %	276 F/g at 0.5 A/g	100.5	4,353	Guo et al. (2016)
Foxtail grass seeds	Distilled water washing	$NaHCO_3$ and $KHCO_3$ activation	2.52 at %	358 F/g at 0.5 A/g	–	–	Liang et al. (2021)
Eucalyptus leaves	Deionized water washing	$KHCO_3$ activation	1.71 at %	372 F/g at 0.5 A/g	–	–	Mondal et al. (2017)

(Continued on following page)

TABLE 1 (*Continued*) Plant-based N self-doped biochar applications in supercapacitors.

Biomass	Pre-treatment	Preparation method	N content	*C*	*Es* (Wh/kg)	*Ws* (W/kg)	Ref
Fallen flowers of *Magnolia*	–	Pre-carbonization followed by $KHCO_3$ activation	0.97 wt%	302.7 F/g at 0.5 A/g	7.0	100	Qi et al. (2018)
Peanut shell	Washing	Hydrothermal carbonization followed by Na_2CO_3–K_2CO_3 activation	1.02 at %	447 F/g at 0.2 A/g	12.75	50	Lei et al. (2021)
Pine pollen	–	$MgCO_3$ activation	3.13 at %	419.6 F/g at 1 A/g	34.9	181	Wan et al. (2019)
Lily	Ethanol/deionized water washing	$KMnO_4$ hot solution treatment followed by carbonization	3.31 at %	352 F/g at 0.5 A/g	23.82	700	Wang et al. (2022)
Spring onion peel	Ethanol/deionized water washing	$KMnO_4$ hot solution treatment followed by carbonization	1.1 at %	490.7 F/g at 1 A/g	92	1800	Zhao et al. (2020)
Clover	–	Hydrothermal treatment with KCl followed by carbonization	2.59 at %	451 F/g at 0.5 A/g	10.7	125	Wang et al. (2018)
Clover	–	KOH activation	2.55 at %	436 F/g at 1 A/g	58.4	500	Wang et al. (2017)
Flower petals of *Salvia splendens*	Ethanol/deionized water washing	Impregnation with NaCl followed by carbonization	2.32 at %	294 F/g at 1 A/g	20.9	467.9	Liu et al. (2018)
Chestnut	–	Pre-carbonization followed by KOH activation	2.63 wt%	160 F/g at 1 A/g	3.12	2030	Januszewicz et al. (2020)
Carrots	–	Na_2SiO_3 activation	3.4 at %	268 F/g at 1 A/g	–	–	Du et al. (2021)
Celery	Washing	Direct pyrolysis	2.5 at %	245 F/g at 1 A/g	10.12	225.7	He et al. (2019)
Kapok fiber	NaOH solution/ deionized water washing	Direct pyrolysis	0.76 wt%	283 F/g at 1 A/g	–	–	Wang et al. (2018)
Perilla frutescens leaves	Ultrapure water washing	Direct pyrolysis	1.7 at %	270 F/g at 0.5 A/g	14.8	490	Liu et al. (2017)

C is the maximum specific capacitance of N self-doped biochar in a three-electrode system.
Es and *Ws* are the maximum energy density and power density of the assembled supercapacitor, respectively.

foamed and activated in $KMnO_4$ hot solution, obtaining an N, O co-doped porous carbon material with a specific capacitance of 352 F/g at 0.5 A/g (Wang et al., 2022). $KMnO_4$ was also employed as the activating reagent for spring onion peel-derived biochar (Zhao et al., 2020), the specific capacitance of which was 490.7 F/g at 1.0 A/g and the energy density was 92.0 Wh/kg at a power density of 1800 W/kg in supercapacitors. KCl and NaCl were utilized as activators when producing N self-doped biochar from clover (Wang et al., 2017; Wang et al., 2018) and flower petals of *Salvia splendens* (Liu et al., 2018).

A comparison of KOH and other activating reagents was also performed. For example, chemically and physically activated pyrolysis of chestnut was compared using KOH and CO_2 as activators, respectively (Januszewicz et al., 2020). The KOH-activated sample exhibited much better electrochemical performance due to the higher SSA and well-developed porosity. N self-doped porous carbons were synthesized using vitamin-enriched carrots and an Na_2SiO_3 activator (Du et al., 2021). Na_2SiO_3 showed a better activation performance than KOH, leading to a high capacitance of 268 F/g at 1 A/g for the derived biochar.

Without using any activating reagents, He et al. reported an N self-doped biochar obtained from the direct calcination of celery, the capacitance of which reached 245 F/g (He et al., 2019). Kapok fiber (Wang et al., 2018) and *Perilla frutescens* (Liu et al., 2017) were also directly pyrolyzed to synthesize an N self-doped biochar for supercapacitors.

3.2 Animal-based N self-doped biochar

The preparation and application of animal-based N self-doped biochar in supercapacitors are summarized in Table 2. Waste shrimp shells that contain N-rich poly-b (1/4)-N-acetyl-D-glucosamine were expected to be an excellent precursor for N self-doped carbon. For example, shrimp shell-derived carbon using hydrothermal treatment with KOH and carbonization obtained a specific capacitance of 239 F/g at 0.5 A/g (Mondal et al., 2017). Mantis shrimp shells were directly carbonized at different temperatures, and the biochar derived at 750 °C demonstrated a high specific capacitance of 201 F/g at a current density of 1 A/g due to the large SSA of 401 m^2/g and high N content (8.2 wt%) (Huang et al., 2021).

TABLE 2 Animal-based N self-doped biochar applications in supercapacitors.

Biomass	Pre-treatment	Preparation method	N content	C_{max}	E_s (Wh/kg)	W_s (W/kg)	Reference
Shrimp shells	Deionized water washing	Hydrothermal treatment with KOH followed by carbonization	2.86%	239 F/g at 0.5 A/g	–	–	Mondal et al. (2017)
Mantis shrimp shell	Deionized water washing	Direct pyrolysis	8.2 wt%	201 F/g at 1 A/g	–	–	Huang et al. (2021)
Cattle bone	–	Pre-carbonization followed by KOH activation	2.3%	240 F/g at 5 A/g	75	3,750	Shao et al. (2017)
Cattle bone	–	Pre-carbonization followed by KOH activation	1.56%	435 F/g at 0.1 A/g	30.3	341	He et al. (2017)
Blackfish bone	Ethanol washing	KOH activation	6.3 at %	302 F/g at 0.5 A/g	7	300	Niu et al. (2019)
Silkworm cocoon	–	Phytic acid activation	3.65%	317 F/g at 1 A/g	19.6	350	Wang et al. (2019)
Beehive	–	KOH activation	7.3 at %	296.1 F/g at 1 A/g	–	–	Wang et al. (2020)
Human hair	Deionized water washing	Pre-carbonization followed by KOH activation	3.16 at %	999 F/g at 1 A/g	32	325	Sinha et al. (2020)
Fish skin	Deionized water washing	Hydrothermal treatment with KOH followed by carbonization	8.18%	438 F/g at 0.1 A/g	12.5 Wh/L	24 W/L	Niu et al. (2018)
Pig nail	Deionized water washing	Pre-carbonization followed by KOH activation	2.1 at %	251.4 F/g at 1 A/g	29.43	847.9	Tang et al. (2019)
Natural casing	Deionized water washing	Pre-carbonization followed by KOH activation	6.34 at %	307.5 F/g at 0.5 A/g	11.6	297	Xu et al. (2018)
Porcine bladders	Deionized water washing	Pre-carbonization followed by KOH activation	5.38%	322.5 F/g at 0.5 A/g	10.9	150	Wang et al. (2019)

Animal bone is a natural composite composed of organic collagen. It is rich in C/N elements and can be used as the C/N source to form N self-doped carbons. It is also a source of inorganic hydroxyapatite that disperses homogeneously within the bone as a natural template (Shao et al., 2017). The cattle bone-derived carbon possessed an ultrahigh SSA (2,203 m^2/g) with meso- and macropores, a high N content (2.3%), and a good specific capacitance (Shao et al., 2017). He et al. reported an N/O co-doped carbon from cattle bones with a large SSA (2,520 m^2/g), a high content of N (1.56%) and O (10.2%), and a large specific capacity (435 F/g at 0.1 A/g) (He et al., 2017). By simultaneous pyrolysis and activation, pork bone, blackfish bone, and eel bone-derived carbon, which had a higher ratio of micropore surface area and N content, exhibited enhanced specific capacitance (Niu et al., 2019).

N/P co-doped porous carbon was prepared from silkworm cocoons and phytic acid by the self-activation approach, achieving a gravimetric capacitance of 317 F/g at 1 A/g (Wang et al., 2019). After sufficient soaking with KOH solution, the beehive was then calcined to produce a multilevel gradient structural N/S co-doped carbon (Wang et al., 2020). The obtained carbon materials exhibited a best capacitive capability of 296.1 F/g at a current density of 1 A/g. Human hair, rich in keratin, was carbonized with KOH, $ZnCl_2$, and H_3PO_4. The KOH-activated biochar showed the best electrochemical performance with an outstanding specific capacitance of 999 F/g at a current density of 1 A/g (Sinha et al., 2020). After treatment with KOH, fish skin, primarily composed of collagen, such as glycine, proline, alanine, and methionine, was converted into ternary-doped carbon nanosheets (Niu et al., 2018), with a gravimetric capacitance of 438 F/g at 0.1 A/g. Using pig nail as N-rich biomass, a porous carbon was fabricated by carbonization and KOH activation. The supercapacitor derived from this product exhibited a remarkable energy density of 29.43 Wh/kg (Tang et al., 2019). An N-enriched biochar was fabricated from the natural casing, an inherently tough translucent film consisting of fat and protein, and exhibited a desirable SSA (3,100 m^2/g), high N content (6.34 at.%), and high specific capacitance (307.5 F/g at 0.5 A/g) (Xu et al., 2018). Porcine bladders were also processed with the same strategy (Wang et al., 2019). The derived carbon material exhibited large SSA (1881.7 m^2/g), high N content (5.38%), and, consequently, high specific capacitance (322.5 F/g at 0.5 A/g).

3.3 Food-based N self-doped biochar

Eggs, beancurd, and milk, which are rich in protein and can be used as human food, are assigned to N-rich food-based biomass. Table 3 shows the details of the preparation and application of food-based N self-doped biochar in supercapacitors. A two-step method involving carbonization and KOH activation was employed to synthesize carbon materials from egg white (Zhu et al., 2019). The derived carbon showed a high SSA of 2,918 m^2/g and a high

TABLE 3 Food-based N self-doped biochar applications in supercapacitors.

Biomass	Pre-treatment	Preparation method	N content	C_{max}	E_s (Wh/kg)	W_s (W/kg)	Reference
Egg white	–	Pre-carbonization followed by KOH activation	–	335 F/g at 0.5 A/g	13.6	300	Zhu et al. (2019)
Egg white	–	Pyrolysis with ZnO template	6.22%	205 F/g at 0.5 A/g	–	–	Chen et al. (2015)
Chicken eggs	–	Hydrothermal treatment with graphene oxide followed by KOH activation	5.76 at %	482 F/g at 0.1 A/g	11.3	25	Ma et al. (2017)
Milk	–	Hydrothermal carbonization followed by sequential KOH–H_3PO_4 activation	–	186.3 F/g at 0.9 A/g	–	–	Dat et al. (2020)
Yogurt	–	Hydrothermal treatment followed by KOH activation	12 wt%	225 F/g at 2 A/g	27	364	Wahid et al. (2015)
Soybean milk	–	Carbonization with KOH and $CaCO_3$	2.4%	240.7 F/g at 1 A/g	10.2	351	Chen et al. (2019)
Beancurd	–	Pre-carbonization followed by CH_3COOK activation	1.33 at %	315 F/g at 0.1 A/g	–	–	Li et al. (2019)
Beancurd	–	CH_3COOK activation	2.62 at %	284 F/g at 0.1 A/g	–	–	Li et al. (2018)
Coffee	–	Water vapor activation	4.5 at %	312F/g at 1.0 A/g	27.8	1820	Zhang et al. (2022)

specific capacitance of 335 F/g at 0.5 A/g. Egg white was also carbonized with a ZnO template to fabricate a carbon material with a capacitance of 205 F/g at 0.5 A/g (Chen et al., 2015). Ma et al. reported an N self-doped carbon from the mixture of fresh chicken eggs and graphene oxide *via* hydrothermal carbonization and KOH activation (Ma et al., 2017).

Dat et al. (2020) prepared an N self-doped carbon from expired fresh milk *via* hydrothermal carbonization and sequential KOH–H_3PO_4 activation. The derived biochar achieved a specific capacitance of 186.3 F/g. Yogurt was also used to synthesize highly N self-doped biochar for supercapacitor application *via* hydrothermal treatment and activation (Wahid et al., 2015). A strategy of simultaneous $CaCO_3$ template and KOH activation was explored for N self-doped biochar production from soybean milk (Chen et al., 2019). The obtained carbons exhibited a specific capacitance of 240.7 F/g at 1 A/g.

A one-step impregnation activation method (Li et al., 2018) and a two-step method with the CH_3COOK activator (Li et al., 2019) were reported for N self-doped biochar synthesis from beancurd. CH_3COOK was decomposed into K_2CO_3 at about 303 °C and then as-formed K_2CO_3 reacted with carbon to generate many micropores, following R2-R5. The derived carbon materials delivered capacitances of 284 F/g and 245 F/g, respectively, at 0.1 A/g.

Zhang et al. reported an N, O-doped activated carbon from household expired coffee by direct water vapor activation, achieving a high gravimetric capacitance of 312 F/g at 1.0 A/g (Zhang et al., 2022).

3.4 Algae-based N self-doped biochar

Algae are autotrophic and embryoless plants capable of photosynthesis involving macroalgae and microalgae, which are mainly composed of lipids, proteins, and carbohydrates (Sun et al., 2022). It was reported that a hierarchically porous structure with a balanced distribution of mesopores and micropores is more effective in the capacitive performance of algae-derived carbon than the components of raw algae, such as proteins (Zhu et al., 2018). Therefore, the synthesis of N self-doped char with a well-developed pore structure is a promising pathway for algae utilization. The algae-based N self-doped biochar in supercapacitor results are presented in Table 4.

A two-step procedure of carbonization and KOH activation was used for biocarbon preparation from *Lessonia trabeculata* (Sankaranarayanan et al., 2021) and *Laminaria japonica* (Cheng et al., 2020). The derived carbon materials exhibited good capacitances of 81.6 F/g at 1A/g and 192 F/g at 0.1 A/g, respectively. *Chlorella*-derived activated carbon was also prepared *via* the two-step procedure, exhibiting a gravimetric specific capacitance of 142 F/g at 1 mA/cm^2 (Han et al., 2019). Ren et al. reported an N self-doped carbon from hydrothermal carbonization of *Enteromorpha prolifera*, followed by a mild KOH activation (Ren et al., 2018). *Ascophyllum nodosum* (Perez-Salcedo et al., 2020), *Cladophora glomerata* (Norouzi et al., 2021), and *Enteromorpha* (Yu et al., 2016) were also activated by KOH to fabricate N self-doped carbon material for supercapacitor application. Immersion with hydrofluoric acid increased the electrochemical performance of the biochar from *Nostoc flagelliforme* algae (Wang et al., 2019).

Three types of marine algae were carbonized at 800 °C with *in situ* salts as activating reagents (Gao et al., 2021). The derived biochar possessed high SSA (621–1,140 m^2/g) and N content (4.15–5.19%) and exhibited good energy storage performance (190.0–278.5 F/g at 0.5 A/g) and cyclic stabilities (96%–98% after 5,000 cycles). *Chlorella* mixed with reed and K_2CO_3 was carbonized to produce 3D N-doped biochar (Yuan et al., 2022). Due to the high N content (2.1 wt%), large SSA (1794 m^2/g), and pore volume (1.32 cm^3/g), the capacitance of the biochar reached 340.4 F/g at 1 A/g. Liu et al. reported a sponge-like carbon material from

TABLE 4 Algae-based N self-doped biochar applications in supercapacitors.

Biomass	Pre-treatment	Preparation method	N content	C_{max}	E_s (Wh/kg)	W_s (W/kg)	Ref
Lessonia trabeculata	–	Pre-carbonization followed by KOH activation	0.5 at %	81.6 F/g at 1 A/g	–	–	Sankaranarayanan et al. (2021)
Laminaria japonica	–	Pre-carbonization followed by KOH activation	0.47 at %	192 F/g at 0.1 A/g	–	–	Cheng et al. (2020)
Enteromorpha prolifera	Deionized water washing	Hydrothermal treatment and carbonization followed by KOH activation	1.4 at %	214 F/g at 0.1 A/g	–	–	Ren et al. (2018)
Ascophyllum nodosum	Washing	Impregnation with KOH followed by carbonization	0.8 wt%	207.3 F/g at 0.5 A/g	–	–	Perez-Salcedo et al. (2020)
Enteromorpha	Deionized water washing	Impregnation with KOH followed by carbonization	0.85 at %	201 F/g at 1 A/g	62	680–750	Yu et al. (2016)
Nostoc flagelliforme	Ac–H_2O_2/Ac-$NaClO_2$/HF washing followed by deionized water washing	Pre-carbonization followed by KOH activation	–	283 F/g at 0.1 A/g	22	80	Wang et al. (2019)
Kelp	–	Direct pyrolysis	4.15%	278.5 F/g at 0.5 A/g	5.24	123.8	Gao et al. (2021)
Chlorella	–	K_2CO_3 activation of *Chlorella* and reed mixture	2.1 wt%	340.4 F/g at 1 A/g	23.6	15,000	Yuan et al. (2022)
Spirulina platensis	–	$NaHCO_3$ activation	7.5 wt%	234 F/g at 1 A/g	–	–	Liu et al. (2018)
Myriophyllum aquaticum	–	$KHCO_3$ activation	2.3 at %	248.2 F/g at 0.5 A/g	–	–	Shen et al. (2018)

Spirulina platensis with $NaHCO_3$ activation, the largest specific capacitance of which was 234 F/g at 1 A/g (Liu et al., 2018). A comparison between $KHCO_3$ and CO_2 activation was conducted for *Myriophyllum aquaticum*-derived biochar production (Shen et al., 2018). The results showed that the $KHCO_3$-activated carbon possessed a better electrochemical performance.

3.5 Organic waste-based N self-doped biochar

N-rich organic wastes are by-products with high N content generated during the industrial manufacturing process, such as antibiotic fermentation residue from antibiotic production, spent coffee ground from coffee brewing, bean pulp/oil cake from oil production, and composting leachate from biobased-waste composting. The application of organic waste-based N self-doped biochar in supercapacitors is summarized in Table 5.

Antibiotic fermentation residue, which is inevitably produced during the antibiotic fermentation process, can be used for N self-doped biochar production due to its high N content and large volume. The oxytetracycline mycelial residue-derived biochar *via* carbonization and KOH activation showed an ultrahigh SSA (2,574.9 m^2/g), a higher N content (2.27%), and, consequently, a distinguished specific capacitance (307 F/g) (Zhang et al., 2021). Chen et al. (2022) fabricated self-doped porous carbon nanosheets from fermentation residues of lincomycin hydrochloride *via* high-temperature pyrolysis and subsequent KOH activation. The derived biochar exhibited an excellent gravimetric capacitance of 296 F/g at 1 A/g. Hu et al. (2022) reported an N self-doped porous carbon from penicillin fermentation residue *via* hydrothermal carbonization combined with KOH or $ZnCl_2$ activation. The $ZnCl_2$-activated biochar exhibited a larger SSA of 792.58 m^2/g and a higher N content of 4.75%, resulting in a higher specific capacitance of 209.2 F/g at 1 A/g in a three-electrode system and an energy density of 8.79 Wh/kg for assembled supercapacitors.

N self-doped biochar was synthesized from spent coffee grounds *via* hydrothermal carbonization, followed by KOH activation (Sangprasert et al., 2022). The optimal biochar showed a high SSA of 1835 m^2/g and 2.35 wt% N content, and, subsequently, a high energy density of 10.84 Wh/kg in a two-electrode system. A procedure of hydrothermal acidic hydrolysis, followed by KOH activation was also designed for spent coffee ground biochar production for use in supercapacitors (Biegun et al., 2020).

The high protein content in the defatted soybean, a solid residue generated from oil production, makes it highly suitable for the fabrication of N self-doped carbon materials. Zhou et al. reported an N/O co-doped porous carbon from soybean dregs through carbonization and KOH activation, possessing a high SSA (1837.26 m^2/g) and a high N content (1.58 wt%), and then a superior specific capacitance (Zhou et al., 2018). Another procedure of hydrothermal carbonization and KOH activation was implemented to convert soybean residue into an N self-doped carbon with high specific capacitance (Ferrero et al., 2015). By carbonization and CO_2 activation, bean pulp was converted into a carbon material with a maximum SSA of 558.2 m^2/g, an N content of up to 10%, and a maximum specific capacitance of 106 F/g at 0.25 A/g (Ding et al., 2021). The

TABLE 5 Organic waste-based N self-doped biochar applications in supercapacitors.

Biomass	Pre-treatment	Preparation method	N content	C_{max}	E_s (Wh/kg)	W_s (W/kg)	Reference
Oxytetracycline mycelial residues	–	Pre-carbonization followed by KOH activation	2.27%	307 F/g at 0.5 A/g	–	–	Zhang et al. (2021)
Penicillin fermentation residue	–	Hydrothermal treatment followed by $ZnCl_2$ activation	4.75 wt%	209.2 F/g at 1 A/g	8.79	–	Hu et al. (2022)
Fermentation residues	–	Pre-carbonization followed by KOH activation	4.3 at %	345 F/g at 1 A/g	173	1900	Chen et al. (2022)
Spent coffee grounds	–	Hydrothermal treatment with acetic acid, followed by KOH activation	1.2 at %	246 F/g at 1 A/g	10.84	4,589	Sangprasert et al. (2022)
Spent coffee grounds	–	Hydrothermal treatment, pre-carbonization, and KOH activation	–	178.0 F/g at 50 A/g	84	202,000	Biegun et al. (2020)
Soybean dregs	–	Pre-carbonization followed by KOH activation	1.58 at %	321.1 F/g at 1 A/g	22.1	875	Zhou et al. (2018)
Soybean residue	–	Hydrothermal treatment followed by KOH activation	1.6 wt%	261 F/g at 0.2 A/g	12	2000	Ferrero et al. (2015)
Bean pulp	–	Pre-carbonization followed by CO_2 activation	10%	106 F/g at 0.25 A/g	–	–	Ding et al. (2021)
Oil cake	Washing	K_2FeO_4 carbonization	1.99 at %	250.8 F/g at 1 A/g	6.4	100	Yao et al. (2021)
Composting leachate	–	Hydrothermal pre-carbonization and KOH activation	2.35%	228 F/g at 0.5 A/g	7.1	124.9	Liu et al. (2020)
Footwear leather wastes	Ethanol washing	Pre-carbonization followed by KOH activation	12.4 wt%	268 F/g at 5 mV/s	12.8	1800	Martínez-Casillas et al. (2018)
PTM bark waste	Deionized water washing	Pre-carbonization followed by $ZnCl_2$ activation	3.0 wt%	206 F/g at 0.5 A/g	–	–	Sun (2017)

introduction of CO_2 retained more N atoms in biochar in the form of N-5, N-6, N-Q, and N-X. Oil cake, the main by-product of *Idesia polycarpa* oil production, also contributed to N self-doped porous biochar with K_2FeO_4 impregnation and activation (Yao et al., 2021). During the impregnation process, K_2FeO_4 was hydrolyzed into KOH and $Fe(OH)_3$ (R6). The activation process of KOH is described in R1-R5, and that of $Fe(OH)_3$ is shown in R7-R9. First, $Fe(OH)_3$ was transformed into Fe_2O_3 and then further reduced to Fe_3O_4 by carbon or reductive gases (H_2, CO). Then, Fe_3O_4 was further reduced into metallic Fe, which finally catalyzed the conversion of amorphous carbon into graphitized carbon.

$$4K_2FeO_4 + 10H_2O \rightarrow 8KOH + 4Fe(OH)_3 + 3O_2 \quad (R6)$$

$$Fe(OH)_3 \rightarrow FeO(OH) \rightarrow Fe_2O_3 \quad (R7)$$

$$3Fe_2O_3 + (C, H_2, CO) \rightarrow 2Fe_3O_3 + (H_2O, CO, CO_2) \quad (R8)$$

$$Fe_3O_4 + 4(C, H_2, CO) \rightarrow 3Fe + 4(H_2O, CO, CO_2) \quad (R9)$$

Composting leachate, a type of organic wastewater produced during composting of biobased waste, mainly consists of oxidizable organics, ammonium, phosphorus, and pathogenic organisms. Due to its high moisture content, a hydrothermal pre-carbonization and KOH activation strategy was used to produce carbon materials for supercapacitors (Liu et al., 2020). The carbon material exhibited the highest SSA of 2,184.9 m^2/g and an excellent capacitance of 228 F/g at 0.5 A/g.

Footwear leather waste generated from the cutting process of footwear manufacturing was also contributed to N self-doped biochar production. After carbonization and KOH activation, the leather-derived biochar obtained a specific capacitance of 268 F/g (Martínez-Casillas et al., 2018). N self-doped carbon materials (3.0 wt%) prepared from the waste of PTM bark generated from Xuan paper manufacturing exhibited a high specific capacitance of 206 F/g at 0.5 A/g (Sun, 2017).

3.6 Protein/amino acid-based N self-doped biochar

As green, highly accessible, and eco-friendly organic compounds, proteins and amino acids can not only be used as dopants of N atoms but also the precursor of both carbon and nitrogen directly to prepare N self-doped carbon materials. The application of protein/amino acid-based N self-doped biochar is shown in Table 6.

Using soy protein as a C/N precursor, N/O co-doped carbon coated graphene was prepared by one-pot hydrothermal synthesis, followed by carbonization (Xie et al., 2019). The resultant material demonstrated a high volumetric capacitance of 221 F/g at 0.2 A/g. Another N/O co-doped carbon was fabricated from pea protein, the specific capacitance of which reached 413 F/g at 1 A/g (Demir et al., 2018). Microporous carbon obtained from protein by KOH activation (Niu et al., 2019) exhibited an SSA of 1,117 m^2/g, a high N content of 15.29 at.%, and a specific capacitance up to

336 F/g at 1 A/g. N self-doped porous carbons were synthesized for supercapacitor application from sericin, a waste protein (Song et al., 2018). Ma et al. reported a beer yeast protein-derived carbon *via* stepwise pyrolysis without an activator (Ma et al., 2019). Wheat gluten, a complex mixture of hundreds of proteins found in wheat and related grains (Xu et al., 2018), and electrospun plant protein fibers (Yang et al., 2018) were also converted into N self-doped porous carbon for supercapacitor application.

There are many different kinds of amino acids with low price, abundance, accessibility, and low health use for N self-doped biochar fabrication. For example, the N self-doped carbon prepared from L-glutamic acid with $ZnCl_2$ activation exhibited a specific capacitance of 330.6 F/g at 1 A/g (Ma et al., 2016). N/S co-doped carbons were prepared by KOH carbonization of the combination of L-cysteine and NaCl template at 600 °C–800 °C (Guo et al., 2021). Due to the highest N content, the 700 °C-derived biochar showed the largest gravimetric capacitance of 363.1 F/g.

3.7 Fungus-based N self-doped biochar

By pyrolyzing *Flammulina velutipes* pickled with $Mg(CH_3COO)_2$, a self-doped biochar with an SSA of 1,174.2 m^2/g and an N content of 3.97 at% was obtained, showing a specific capacitance of 470.5 F/g at 0.5 A/g (Xue et al., 2022). The $FeCl_3$-activated mushroom-derived biochar exhibited larger SSA, higher N content, and better electrochemical performance than those activated by KOH (Hou et al., 2019). With the activation of KOH or $ZnCl_2$, the *Bacillus subtilis*-derived carbon exhibited superior performance in capacitors (Zhu et al., 2013). Bamboo fungus (Zou et al., 2019) and fresh *Agaricus* (Wang and Liu, 2015) were also converted into N-doped carbon using a two-step procedure of carbonization and KOH activation, offering good specific capacitances. The natural spores of *Lycoperdon boavista* were directly pyrolyzed at 800 °C, and the derived biochar showed a capacity of 260 F/g at 5 A/g (Sun et al., 2020). The details of the fungus-based N self-doped biochar application in a supercapacitor are presented in Table 7.

3.8 Other N self-doped biochars

Gelatin is an animal derivative composed of various proteins. It is produced by partial hydrolysis of collagen extracted from the skin, bones, and connective tissues of animals (Xu et al., 2014). By successive pyrolysis with citric acid and anhydrous iron (III) chloride, gelatin was converted into an N/O co-doped porous carbon with a specific capacitance of 312 F/g at 1 A/g (Shi et al., 2017). The mixture of gelatin and KNO_3 was also annealed for the synthesis of the N self-doped carbon used in supercapacitors (Deng et al., 2020).

Chitin, a polysaccharide substance extracted from the shell of marine crustaceans, also contributes to N self-doping. For example, chitin was carbonized with $CuCl_2.2H_2O$ to prepare a natural structure-maintained O/N-enriched biochar (Luo et al., 2020). Reactions between the chitin and $CuCl_2.2H_2O$ were confirmed according to the evident differences that appeared in thermogravimetry/differential thermogravimetry (TG)/(DTG) curves ranging from 450 to 750°C between the mixture of chitin and $CuCl_2.2H_2O$ (Figure 8A) and individual chitin (Figure 8B). The obtained biochar exhibited an SSA range of 1,635–2,381 m^2/g, a tunable micropore volume ratio of 63.5–96.8%, and high O/N contents (N: 3.1–9.0 wt% and O: 10.5–12.8 wt%), resulting in a high specific capacitance of 286 F/g at 0.5 A/g. Raj et al. also reported an O/N co-doped carbon from squid gladius chitin, achieving a maximum specific capacitance of 204 F/g (Raj et al., 2018).

N self-doped carbon material was synthesized directly from chitosan using a hydrothermal treatment, followed by KOH activation for supercapacitor application (Zhu et al., 2017). The synthesized carbon exhibited high SSA (2,200 m^2/g), large pore volume (1.36 cm^3/g), and high N content (6.3%), resulting in a specific capacitance of 305 F/g at 0.5 A/g in 6 M KOH electrolytes. Simultaneous carbonization and KOH activation of chitosan regenerated from prawn shells also resulted in an N self-doped biochar with a high specific capacitance of 357 F/g at 50 mA/g (Gao et al., 2016).

Activated carbon with high SSA (1841 m^2/g) and N self-inherited (2.1 at%) were obtained from *Artocarpus heterophyllus* seed-derived starch with $ZnCl_2$ activation (Kasturi et al., 2019). N-doped carbon nanosheets were prepared *via* simultaneous activation and graphitization of biomass-derived natural silk (Hou et al., 2015). Due to the resulting product's high SSA (2,494 m^2/g), high volume of hierarchical pores (2.28 cm^3/g), and rich N-doping (4.7%), the as-obtained carbon exhibited a capacitance of 242 F/g. The results of the other N self-doped biochars in a supercapacitor are given in Table 8.

4 Evolution of N-functionalities during N self-doped biochar production

The N in the raw biomass mainly occurs in the form of protein-N/amino acid (N-A, 399.9 ± 0.2 eV), which occupies 60%–100% of the total N. During pyrolysis, N-A is quite easily converted to incondensable gas (NH_3, HCN, HNCO, NO, and N_2), condensable organic components (amine-N, nitrile-N, and heterocyclic-N), and more stable N-functionalities in biochar (Zhu et al., 2016; Zhan et al., 2018; Liu et al., 2019). Four types of N-functionalities involving pyrrolic N (N-5, 400.5 ± 0.3 eV), pyridinic N (N-6, 398.8 ± 0.2 eV), quaternary-N (N-Q, 401.4 ± 0.2 eV), and oxidized N (N-X, 402–405 eV) are found to exist in biochar by XPS, as shown in Figure 9 (Zhang et al., 2021). For the carbons derived from most types of biomass, N-5 and N-6 are the dominant N-functionalities, contributing more than half of the total N content (Shen et al., 2018; Yang et al., 2018; Lian et al., 2019; Wan et al., 2019; Wang et al., 2019; Sun et al., 2020). Distinctively, N-Q was the most abundant N-functionality in cattle bone-derived biochar (Shao et al., 2017) and amino acid-derived biochar (Gao et al., 2016).

It was reported that the N content in the raw biomass and the pyrolysis temperature had a crucial effect on N distribution in biochar (Liu et al., 2019). The biochar produced from N-richer biomass also has a higher N content (Leng et al., 2020; Xu et al., 2021). Therefore, the N content of biochar can be expected to be regulated by the selection of raw material. However, biomass type

TABLE 6 Protein/amino acid-based N self-doped biochar applications in supercapacitors.

Biomass	Pre-treatment	Preparation method	N content	*C*	E_s (Wh/kg)	W_s (W/kg)	Reference
Soy protein	–	Hydrothermal treatment with graphene oxide and NaOH, followed by carbonization	3.7 at %	221 F/g at 0.2 A/g	–	–	Xie et al. (2019)
Pea protein	–	Pre-carbonization followed by KOH activation	2.5 at %	413 F/g at 1 A/g	–	–	Demir et al. (2018)
Protein	–	Pre-carbonization followed by KOH activation	15.29 at %	336 F/g at 1 A/g	27	900	Niu et al. (2019)
sericin	–	Pre-carbonization followed by KOH activation	2.28 wt%	287 F/g at 0.5 A/g	6.13	–	Song et al. (2018)
Beer yeast protein	–	Pre-carbonization and deep pyrolysis	–	300 F/g at 1 A/g	13.3	399	Ma et al. (2019)
Wheat gluten	–	Hydrothermal treatment followed by KOH activation	1.93 at %	350 F/g at 0.5 A/g	47	374	Xu et al. (2018)
Electrospun plant protein fibers	–	Carbonization with calcium acetate	6.4%	223.4 F/g at 0.5 A/g	–	–	Yang et al. (2018)
L-glutamic acid	–	$ZnCl_2$ activation	7.1%	330.6 F/g at 1 A/g	16.7	404.7	Ma et al. (2016)
L-cysteine	–	Impregnation with NaCl and KOH followed by carbonization	3.13 at %	363.1 F/g at 0.5 A/g	13.4	325	Guo et al. (2021)

TABLE 7 Fungus-based N self-doped biochar applications in supercapacitors.

Biomass	Pre-treatment	Preparation method	N content	*C*	E_s (Wh/kg)	W_s (W/kg)	Reference
Flammulina velutipes	–	Pickled with $Mg(CH_3COO)_2$ followed by carbonization	3.97 at %	470.5 F/g at 0.5 A/g	26	1,000	Xue et al. (2022)
Mushroom	Deionized water washing	Pre-carbonization followed by FeCl3·6H2O activation	3.1 at %	307.4 F/g at 1 A/g	62.6	1,500	Hou et al. (2019)
Bacillus subtilis	–	KOH activation	0.68 at %	310 F/g at 0.2 A/g	–	–	Zhu et al. (2013)
Bamboo fungus	–	Pre-carbonization followed by KOH activation	3.2 at %	228 F/g at 0.5 A/g	4.3	250	Zou et al. (2019)
Agaricus	Deionized water washing	Pre-carbonization followed by KOH activation	2.27 wt%	135 F/g at 5 A/g	–	–	Wang and Liu (2015)
Spores of *Lycoperdon boavista*	–	Direct pyrolysis	20.6 at %	260 F/g at 5 A/g	–	–	Sun et al. (2020)

shows a negligible influence on the distribution of N-functionalities in biochar (Zhan et al., 2018; Liu et al., 2019).

Pyrolysis temperature is most influential to N distribution in biochar. Generally, as temperature increased, the N content continuously decreased, accompanied by the variation of N-functionalities attributing to the decomposition of organic compounds such as proteins. More specifically, N-A was transformed into N-5 and N-6 easily *via* polymerization and rearrangement and completely vanished at lower temperatures (<500 °C), which would then partially convert to more stable N-Q and N-X *via* polycondensation and oxygen reactions as temperature continuously increased (Zhan et al., 2018; Liu et al., 2019). A decrease in N-5 and an increase in N-Q were observed for *Spirulina platensis*-derived N self-doped biochar as the carbonization temperature increased from 600 °C to 800 °C (Liu et al., 2018). Liu et al. (2020) also reported decreases of N-5 and N-6 with activation temperature rising accompanied by the increase of N-Q and N-X. The intensity of N-5 and N-X in beehive-derived biochar was notably reduced as the carbonization temperature increased from 600 °C to 1,000 °C, whereas reserves of N-6 and N-Q were observed (Wang et al., 2020). Moreover, the N content in biochar was found to increase at temperatures lower than 300 °C and then decrease at 400 °C–800 °C (Xu et al., 2021). The decrease of N-content at low temperatures was caused by the dehydration and decarbonization accompanied by the formation of more stable N-functionalities, such as N-5 and N-6, while the decrease is

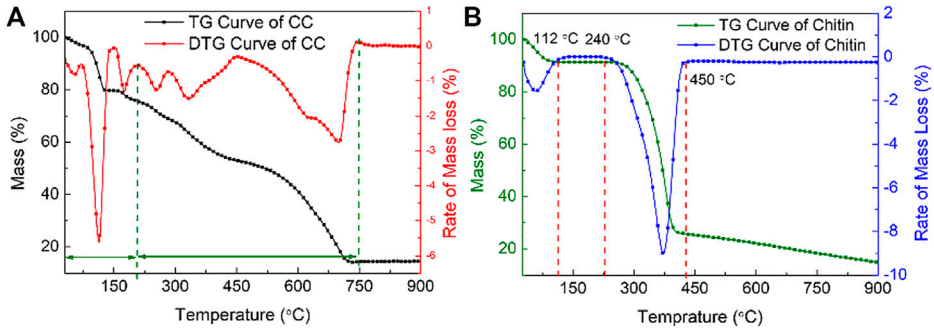

FIGURE 8
(A) TG/DTG curves of a mixture of chitin and $CuCl_2.2H_2O$; **(B)** TG/DTG curves of chitin (Luo et al., 2020).

attributed to the escape of N in the form of un-condensable gas. such as NH_3, HCN, and condensable organic N compounds into the liquid. Nevertheless, the N-5 and N-6 types are reported to be independent of temperature because their percentage was still high, up to 2.1 at.%, even after high-temperature carbonization (Kasturi et al., 2019). Thus, the influence of temperature on N-functionality evolution is still under debate and needs to be further investigated. The introduction of activating reagents would make the evolution pathways more complex. It can be deduced that the N distribution in N self-doped biochar is largely determined by the combined effects of biomass type, pyrolysis temperature, and activating reagent.

Few studies have reported the influences of activating reagents on N distribution in the N self-doped biochar. Generally, the N content of biochar decreased after activation with chemical activators, such as KOH (Ma et al., 2017; Lin et al., 2018; Han et al., 2020; Sankaranarayanan et al., 2021), $KHCO_3$ (Qi et al., 2018), and $Mg(CH_3COO)_2$ (Xue et al., 2022). However, N was found to be more effectively fixed into a carbon skeleton by NaOH (Sattayarut et al., 2019), a eutectic mixture of NaOH/KOH (Zhang et al., 2020), Fe_2O_3 (Wang et al., 2022), or $ZnCl_2$ (Sun, 2017; Han et al., 2018; Hu et al., 2022) activators. Considering the N-functionalities, the N-5 percentage significantly increased with the increasing KOH ratio (Sangprasert et al., 2022). After activation with NaOH, the proportion of N-5, N-6, and N-Q increased, while that of N-X decreased (Sattayarut et al., 2019). Two types of N-functionalities were found in water hyacinth-derived biochar involving N-6 and N-Q (Liang et al., 2018). The content of N-6 increased, while that of N-Q decreased with rising $ZnCl_2$ proportion. NaCl could promote the formation of N-Q and inhibit that of N-5 (Liu et al., 2022). Ding et al. found that the use of CO_2, a typical physical activator, led to more N maintained in biochar, with a decrease of N-6, an increase of N-X, and little influence on N-Q content (Ding et al., 2021). However, CO_2-activated carbons derived from hypha (Lian et al., 2019) and *Ganoderma lucidum* spores (Lian et al., 2019) showed lower N content than the pristine biochar. Compared with $KHCO_3$ activation, CO_2-activated *Myriophyllum aquaticum*-derived biochar exhibited higher N content but fewer types of N-functionalities (Shen et al., 2018).

As an efficient pre-carbonization technique for N self-doped biochar production, hydrothermal treatment also affects the N distribution in the hydrochar. The N content in the hydrochar of *Spirulina* decreased from 17.12% to 0.20% as the temperature increased from 200 °C to 260 °C (Liu et al., 2022) in terms of four types of N-functionalities involving N-6, N-A, N-5, and N-Q. When the temperature was higher than 260 °C, the hydrochar contained almost no N, which was attributed to the extensive cleavage of N-containing macromolecules at a higher temperature into small molecular compounds in the aqueous phase. Nevertheless, as the temperature increased from 180 °C to 250 °C, the N content in seaweed-based hydrochar slightly increased due to the Maillard and Mannich reactions (Soroush et al., 2022). Because the hydrochar often acts as a carbon precursor for subsequent pyrolysis or activation to produce biochar, the variation of N-functionalities in hydrochar will further lead to corresponding changes in N self-doped biochar. For example, evenly mixing with H_3PO_4, pretreatment of durian peel by heating in an oven, and hydrothermal pre-carbonization at 200 °C were compared (Zhou et al., 2020). Hydrothermal pre-carbonization significantly improved the pore structures of the derived biochar (Figures 10A–C). With hydrothermal pre-carbonization, the N content in the biochar decreased, accompanied by N-Q vanishing (Figure 10D). However, the hydrothermal process of carbonized soybean sample showed enhanced N content in the final biochar (Yu et al., 2021).

In addition to the aforementioned factors, pyrolysis pressure (Duan et al., 2017) and pyrolysis programs (Yang et al., 2023) also play effective roles in determining N distribution in biochar. However, to date, N self-doped biochar for supercapacitor application is mainly synthesized under atmospheric pressure with conventional procedures involving one- or two-step methods. Although the types of N-functionalities in N self-doped biochar have been extensively reported by the existing literature, the evolution of N-functionalities in biochar, especially the effects of various activating reagents, is still unclear. More efforts are needed to clarify the impact mechanism of these factors on N-functionality evolution to explore more efficient and novel strategies for N self-doped biochar production.

TABLE 8 Other N self-doped biochar applications in supercapacitors.

Biomass	Pre-treatment	Preparation method	N content	C	E_s (Wh/kg)	W_s (W/kg)	Reference
Gelatin	–	Successive pyrolysis with citric acid and $FeCl_3$	7.03 wt%	312 F/g at 1 A/g	50.2	1,190	Shi et al. (2017)
Gelatin	–	Activation with KNO_3	1.68%	158.9 F/g at 0.5 A/g	88.3	1,000	Deng et al. (2020)
Chitin	–	$CuCl_2{\cdot}2H_2O$ activation	4.5 wt%	286 F/g at 0.5 A/g	15.41	190	Luo et al. (2020)
Squid gladius chitin	–	Pre-carbonization followed by KOH activation	4.04 wt%	204	4.53	9,900	Raj et al. (2018)
Chitosan	–	Hydrothermal treatment followed by KOH activation	1.3%	305 F/g at 0.5 A/g	8.5	1,000	Zhu et al. (2017)
Chitosan	–	KOH activation	4.0 wt%	695 F/g at 50 mA/g	10	1,000	Gao et al. (2016)
Starch	–	$ZnCl_2$ activation	2.1 at %	–	17	810	Kasturi et al. (2019)
Silk	–	Activation with $ZnCl_2$+$FeCl_3$	4.7%	242 F/g at 0.1 A/g	90	875	Hou et al. (2015)

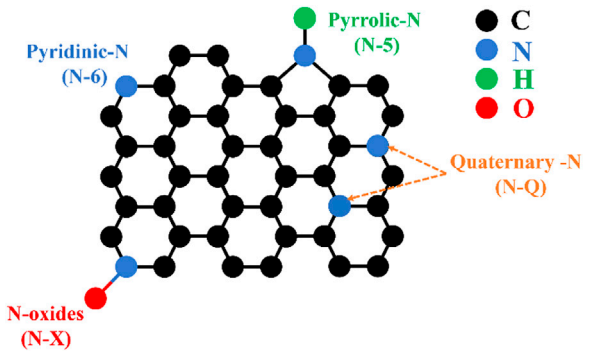

FIGURE 9
Schematic illustration of N functionalities (Zhang et al., 2021).

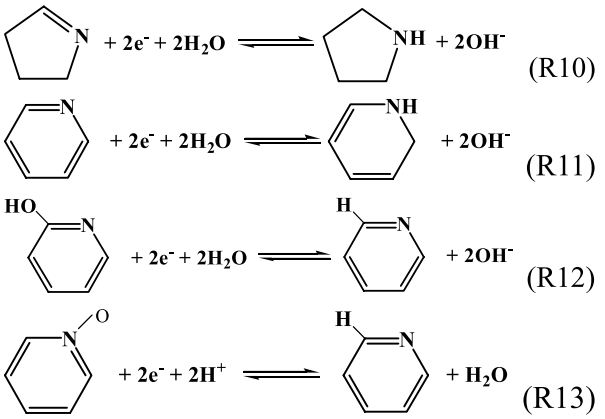

5 Contribution of N-functionalities on supercapacitor performance

There is a consensus that all the N-functionalities contribute to the improvement of supercapacitor performance. Specifically, N-5 and N-6 produce defects in the alkaline electrolyte to provide more open channels and active sites for redox reactions, with electrolyte ions benefitting the pseudo-capacitance (Jiao et al., 2022). R10~R12 are the possible redox reactions of N-5 and N-6 in the KOH electrolyte (Liang et al., 2021). N-Q is the key factor facilitating the charge transfer across the electrode and electrolyte interface and improving the conductivity of carbonaceous materials (Yao et al., 2021). A higher N-X concentration indicates better wettability of the carbon materials (Sangprasert et al., 2022). Wang et al. suggested that N-Xs with high electron affinity and N-6s with less positive charge could generate redox pairs (R13) (Wang et al., 2012).

To quantify the contribution of N self-doping induced pseudo-capacitance to the overall specific capacitance, the N self-doped biochar samples (PFC) from *Perilla frutescens* (PF) leaves were heat-treated for a second time at 900 °C to remove the surface functionalities (Liu et al., 2017). Around 38.8%–46.3% of the specific capacitance was confirmed to be contributed by pseudo-capacitance, as shown in Figure 11. By dividing the corresponding charge by the potential window of CV curves, Xu et al. reported a considerable pseudo-capacitance contribution of 32–40% (Xu et al., 2018). A pseudo-capacitance contribution of 24.7%–41.7% was also estimated for the natural casing-derived carbons (Xu et al., 2018). For the penicillin fermentation residue-derived biochar, N-doping was responsible for 17.87–20.46% of the specific capacitance (Hu et al., 2022). Yao et al. found that the contribution of pseudo-capacitance varied with electrolytes, the values of which were 41.5–83.3%, 12.2–32.6%, and 25.2–45.0% in H_2SO_4, KOH, and Na_2SO_4 electrolytes, respectively (Yao et al., 2021). Deng et al. also reported different pseudo-capacitance contributions in KOH (~28%) and $EMIBF_4$ (16–47.3%) electrolytes (Deng et al., 2020).

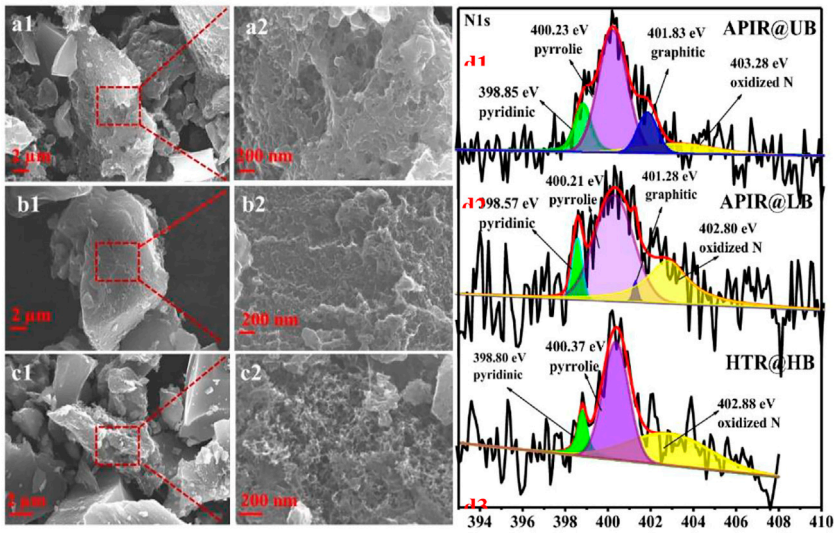

FIGURE 10
(a1, a2) and **(b1, b2)** SEM images of biochar pretreated by heating in an oven at 200 °C, **(c1, c2)** SEM images of biochar pretreated by hydrothermal pre-carbonization at 200 °C, and **(d1-d3)** comparison of N-functionalities between the derived carbons (Zhou et al., 2020).

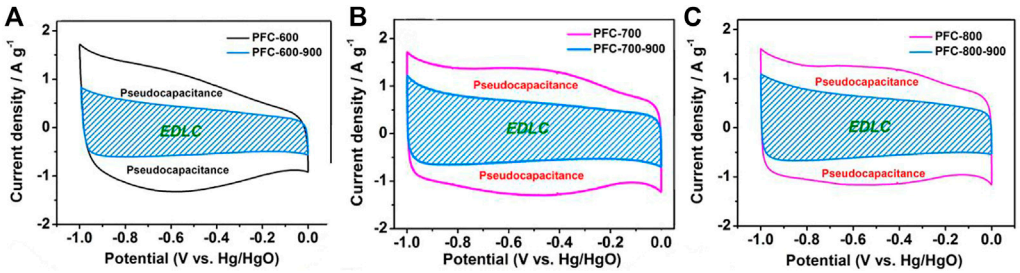

FIGURE 11
CV curves of **(A)** PFC-600 and PFC-600–900, **(B)** PFC-700 and PFC-700–900, and **(C)** PFC-800 and PFC-800–900 (Liu et al., 2017).

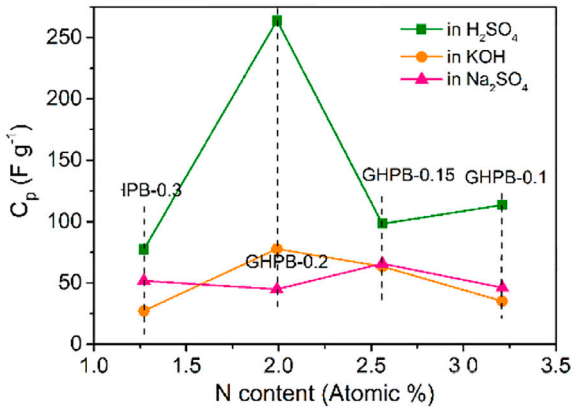

FIGURE 12
Relationship between the specific capacitance and N content (Yao et al., 2021).

However, note that biochar with higher N content is not equal to better electrochemical performance. For example, the *Spirulina platensis* biochar prepared at 600 °C had a higher N content than that prepared at 700 °C, whereas its electrochemical performance was weaker (Liu et al., 2018). Xu et al. also found that the casing-based biochar with the highest N content did not exhibit the best electrochemical performance (Xu et al., 2018). Yao et al. investigated the relationship between the specific capacitance (C_p) and N content of the biochar prepared from oil cake (Yao et al., 2021). As shown in Figure 12, the variations of the curves were extremely irregular, indicating a much more complex relationship between C_p and N content. However, they reported that the pseudo-capacitance contribution was much poorer than that from a sample with superior porosity due to high surface area and suitable pore size. Perez-Salcedo et al. found that the N influence is correlated with porosity (Perez-Salcedo et al., 2020). To date, the relationship between N content and the specific capacitance of N self-doped biochar is still unclear. Research on the interactions of the N functionalities with specific capacitance is unavailable.

It is widely accepted that the electrochemical performance of N self-doped carbon material is mainly determined by the coupling effect of SSA, pore structure, N distribution, *etc.* Although many studies of N self-doped biochar production involving various N-rich biomass and fabrication strategies can be found, the relationship between N content and specific capacitance is still unclear. Due to this, enhancing the electrochemical performance of N self-doped biochar by regulating N content remains challenging. Meanwhile, although the N functionalities of N self-doped biochar have been analyzed in the literature, the connections between them and the specific capacitance are also undiscovered. In particular, the contribution of the N doping-induced pseudo-capacitance to the overall capacitance is rarely reported. Thus, more effort is needed to reveal the impact of N self-doping on the electrochemical performance to provide more information for the tunable fabrication of N self-doped biochar.

6 Conclusion and prospects

This review summarizes the development of N self-doped biochar applications as electrode materials for supercapacitors in the last 10 years. Compared with N-doping with external N precursors, the synthesis of N self-doped biochar from natural N-rich biomass is eco-friendly and cost-efficient. Numerous papers reporting on the preparation and characterization of N self-doped biochar are available, demonstrating the feasibility of N self-doping in improving the electrochemical performance. Some studies have also estimated the contribution of N self-doping-induced pseudo-capacitance to the total specific capacitance. However, it remains challenging to achieve controllable N self-doped biochar with the desired properties because the relationship between the specific capacitance and N self-doping is unclear. It is widely accepted that the electrochemical performance of N self-doped biochar is mainly determined by the combined action of the pore structure, specific surface area, and N distribution, which are primarily influenced by the raw material and the preparation procedures. Therefore, efforts should be devoted to exploring the effect mechanisms of N self-doping on electrochemical performance in the future to provide more fundamental information for regulable N self-doped biochar production.

Author contributions

YH and LX contributed to the conception and design of the review. LX wrote the first draft of the manuscript. YH contributed to the manuscript revision and read and approved the submitted version.

Funding

This review was funded by the Natural Science Foundation of Jiangsu Province (BK20210511) and the National Natural Science Foundation of China Outstanding Youth Program (52125601).

Conflict of interest

The authors declare that the research was conducted in the absence of any commercial or financial relationships that could be construed as a potential conflict of interest.

Publisher's note

References

Bai, P., Liu, W., Yang, C., Wei, S., and Xu, L. (2021). Boosting electrochemical performance of activated carbon by tuning effective pores and synergistic effects of active species. *J. Colloid Interf. Sci.* 587, 290–301. doi:10.1016/j.jcis.2020.12.022

Biegun, M., Dymerska, A., Chen, X., and Mijowska, E. (2020). Study of the active carbon from used coffee grounds as the active material for a high-temperature stable supercapacitor with ionic-liquid electrolyte. *Materials* 13, 3919. doi:10.3390/ma13183919

Bo, X., Xiang, K., Zhang, Y., Shen, Y., Chen, S., Wang, Y., et al. (2019). Microwave-assisted conversion of biomass wastes to pseudocapacitive mesoporous carbon for high-performance supercapacitor. *J. Energy Chem.* 39, 1–7. doi:10.1016/j.jechem.2019.01.006

Cai, Y., Luo, Y., Xiao, Y., Zhao, X., Liang, Y., Hu, H., et al. (2016). Facile synthesis of three-dimensional heteroatom-doped and hierarchical egg-box-like carbons derived from moringa oleifera branches for high-performance supercapacitors. *ACS Appl. Mat. Inter.* 8, 33060–33071. doi:10.1021/acsami.6b10893

Chen, C., Xu, Y., Shao, J., Zhang, Y., Yu, M., Sun, L., et al. (2022). Waste-converted nitrogen and fluorine co-doped porous carbon nanosheets for high performance supercapacitor with ionic liquid electrolyte. *J. Colloid Interf. Sci.* 616, 413–421. doi:10.1016/j.jcis.2022.02.087

Chen, F., Zhang, Y., Zheng, M., Xiao, Y., Hu, H., Liang, Y., et al. (2022). Preparation of high-performance porous carbon materials by citric acid-assisted hydrothermal carbonization of bamboo and their application in electrode materials. *Energy Fuel.* 36, 9303–9312. doi:10.1021/acs.energyfuels.2c01828

Chen, H., Wang, G., Chen, L., Dai, B., and Yu, F. (2018). Three-Dimensional honeycomb-like porous carbon with both interconnected hierarchical porosity and nitrogen self-doping from cotton seed husk for supercapacitor electrode. *Nanomaterials* 8, 412. doi:10.3390/nano8060412

Chen, J., Liu, Y., Li, W., Yang, H., and Xu, L. (2015). The large electrochemical capacitance of nitrogen-doped mesoporous carbon derived from egg white by using a ZnO template. *RSC Adv.* 5, 98177–98183. doi:10.1039/c5ra15967a

Chen, M., Yu, D., Zheng, X., and Dong, X. (2019). Biomass based N-doped hierarchical porous carbon nanosheets for all-solid-state supercapacitors. *J. Energy Storage* 21, 105–112. doi:10.1016/j.est.2018.11.017

Chen, Q., Sun, J., Wang, Z., Zhao, Z., Zhang, Y., Liu, Y., et al. (2018). Sustainable rose multiflora derived nitrogen/oxygen-enriched micro-/mesoporous carbon as a low-cost competitive electrode towards high-performance electrochemical supercapacitors. *RSC Adv.* 8, 9181–9191. doi:10.1039/C8RA00858B

Cheng, Y., Wu, L., Fang, C., Li, T., Chen, J., Yang, M., et al. (2020). Synthesis of porous carbon materials derived from laminaria japonica via simple carbonization and activation for supercapacitors. *J. Mater. Res. Technol.* 9, 3261–3271. doi:10.1016/j.jmrt.2020.01.022

Cuong, D. V., Matsagar, B. M., Lee, M., Hossain, M. S. A., Yamauchi, Y., Vithanage, M., et al. (2021). A critical review on biochar-based engineered hierarchical porous carbon for capacitive charge storage. *Renew. Sustain. Energy Rev.* 145, 111029. doi:10.1016/j.rser.2021.111029

Dat, N. T., Tran, T. T. V., Van, C. N., Vo, D. N., Kongparakul, S., Zhang, H., et al. (2020). Carbon sequestration through hydrothermal carbonization of expired fresh milk and its application in supercapacitor. *Biomass Bioenergy* 143, 105836. doi:10.1016/j.biombioe.2020.105836

Demir, M., Ashourirad, B., Mugumya, J. H., Saraswat, S. K., El-Kaderi, H. M., and Gupta, R. B. (2018). Nitrogen and oxygen dual-doped porous carbons prepared from pea protein as electrode materials for high performance supercapacitors. *Int. J. Hydrogen Energy* 43, 18549–18558. doi:10.1016/j.ijhydene.2018.03.220

Deng, J., Li, J., Song, S., Zhou, Y., and Li, L. (2020). Electrolyte-dependent supercapacitor performance on nitrogen-doped porous bio-carbon from gelatin. *Nanomaterials* 10, 353. doi:10.3390/nano10020353

Ding, Y., Li, Y., Dai, Y., Han, X., Xing, B., Zhu, L., et al. (2021). A novel approach for preparing *in-situ* nitrogen doped carbon via pyrolysis of bean pulp for supercapacitors. *Energy* 216, 119227. doi:10.1016/j.energy.2020.119227

Du, J., Zhang, Y., Lv, H., and Chen, A. (2021). Silicate-assisted activation of biomass towards N-doped porous carbon sheets for supercapacitors. *J. Alloy. Compd.* 853, 157091. doi:10.1016/j.jallcom.2020.157091

Duan, Y., Duan, L., Anthony, E. J., and Zhao, C. (2017). Nitrogen and sulfur conversion during pressurized pyrolysis under CO2 atmosphere in fluidized bed. *Fuel* 189, 98–106. doi:10.1016/j.fuel.2016.10.080

Ferrero, G. A., Fuertes, A. B., and Sevilla, M. (2015). From Soybean residue to advanced supercapacitors. *Sci. Rep.-UK* 5, 16618. doi:10.1038/srep16618

Foo, K. Y., and Hameed, B. H. (2013). Utilization of oil palm biodiesel solid residue as renewable sources for preparation of granular activated carbon by microwave induced KOH activation. *Bioresour. Technol.* 130, 696–702. doi:10.1016/j.biortech.2012.11.146

Fu, G., Li, Q., Ye, J., Han, J., Wang, J., Zhai, L., et al. (2018). Hierarchical porous carbon with high nitrogen content derived from plant waste (pomelo peel) for supercapacitor. *J. Mater. Sci. Mater. Electron.* 29, 7707–7717. doi:10.1007/s10854-018-8766-0

Gao, F., Qu, J., Zhao, Z., Wang, Z., and Qiu, J. (2016). Nitrogen-doped activated carbon derived from prawn shells for high-performance supercapacitors. *Electrochim. Acta* 190, 1134–1141. doi:10.1016/j.electacta.2016.01.005

Gao, S., Liu, H., Geng, K., and Wei, X. (2015). Honeysuckles-derived porous nitrogen, sulfur, dual-doped carbon as high-performance metal-free oxygen electroreduction catalyst. *Nano Energy* 12, 785–793. doi:10.1016/j.nanoen.2015.02.004

Gao, X., Chen, Z., Yao, Y., Zhou, M., Liu, Y., Wang, J., et al. (2016). Direct heating amino acids with silica: A universal solvent-free assembly approach to highly nitrogen-doped mesoporous carbon materials. *Adv. Funct. Mat.* 26, 6649–6661. doi:10.1002/adfm.201601640

Gao, Y., Sun, R., Li, A., and Ji, G. (2021). *In-situ* self-activation strategy toward highly porous biochar for supercapacitors: Direct carbonization of marine algae. *J. Electroanal. Chem.* 882, 114986. doi:10.1016/j.jelechem.2021.114986

Gopalakrishnan, A., and Badhulika, S. (2020). Effect of self-doped heteroatoms on the performance of biomass-derived carbon for supercapacitor applications. *J. Power Sources* 480, 228830. doi:10.1016/j.jpowsour.2020.228830

Guo, D., Zheng, C., Deng, W., Chen, X. A., Wei, H., Liu, M., et al. (2017). Nitrogen-doped porous carbon plates derived from fallen camellia flower for electrochemical energy storage. *J. Solid State Electr.* 21, 1165–1174. doi:10.1007/s10008-016-3474-2

Guo, N., Li, M., Wang, Y., Sun, X., Wang, F., and Yang, R. (2016). Soybean root-derived hierarchical porous carbon as electrode material for high-performance supercapacitors in ionic liquids. *ACS Appl. Mat. Inter.* 8, 33626–33634. doi:10.1021/acsami.6b11162

Guo, Y., Wang, T., Wu, D., and Tan, Y. (2021). One-step synthesis of *in-situ* N, S self-doped carbon nanosheets with hierarchical porous structure for high performance supercapacitor and oxygen reduction reaction electrocatalyst. *Electrochim. Acta* 366, 137404. doi:10.1016/j.electacta.2020.137404

Han, J., Lee, K., Choi, M. S., Park, H. S., Kim, W., and Roh, K. C. (2019). Chlorella-derived activated carbon with hierarchical pore structure for energy storage materials and adsorbents. *Carbon Lett.* 29, 167–175. doi:10.1007/s42823-019-00018-y

Han, J., Li, Q., Wang, J., Ye, J., Fu, G., Zhai, L., et al. (2018). Heteroatoms (O, N)-doped porous carbon derived from bamboo shoots shells for high performance supercapacitors. *J. Mater. Sci. Mater. Electron.* 29, 20991–21001. doi:10.1007/s10854-018-0244-1

Han, P., Cheng, M., Luo, D., Cui, W., Liu, H., Du, J., et al. (2020). Selective etching of C-N bonds for preparation of porous carbon with ultrahigh specific surface area and superior capacitive performance. *Energy Storage Mater.* 24, 486–494. doi:10.1016/j.ensm.2019.07.009

He, D., Niu, J., Dou, M., Ji, J., Huang, Y., and Wang, F. (2017). Nitrogen and oxygen co-doped carbon networks with a mesopore-dominant hierarchical porosity for high energy and power density supercapacitors. *Electrochim. Acta* 238, 310–318. doi:10.1016/j.electacta.2017.03.218

He, J., Zhang, D., Han, M., Liu, X., Wang, Y., Li, Y., et al. (2019). One-step large-scale fabrication of nitrogen doped microporous carbon by self-activation of biomass for supercapacitors application. *J. Energy Storage* 21, 94.doi:10.1016/j.est.2018.11.015

Hou, J., Cao, C., Idrees, F., and Ma, X. (2015). Hierarchical porous nitrogen-doped carbon nanosheets derived from silk for ultrahigh-capacity battery anodes and supercapacitors. *ACS Nano* 9, 2556–2564. doi:10.1021/nn506394r

Hou, L., Chen, Z., Zhao, Z., Sun, X., Zhang, J., and Yuan, C. (2019). Universal FeCl3-activating strategy for green and scalable fabrication of sustainable biomass-derived hierarchical porous nitrogen-doped carbons for electrochemical supercapacitors. *ACS Appl. Energy Mater.* 2, 548–557. doi:10.1021/acsaem.8b01589

Hu, J., Hong, C., Zhao, C., Si, Y., Xing, Y., Ling, W., et al. (2022). Nitrogen self-doped hierarchical porous carbon via penicillin fermentation residue (PR) hydrothermal carbonization (HTC) and activation for supercapacitance. *J. Alloy. Compd.* 918, 165452. doi:10.1016/j.jallcom.2022.165452

Huang, G., Wang, Y., Zhang, T., Wu, X., and Cai, J. (2019). High-performance hierarchical N-doped porous carbons from hydrothermally carbonized bamboo shoot shells for symmetric supercapacitors. *J. Taiwan Inst. Chem. E.* 96, 672–680. doi:10.1016/j.jtice.2018.12.024

Huang, S., Ding, Y., Li, Y., Han, X., Xing, B., and Wang, S. (2021). Nitrogen and sulfur Co-doped hierarchical porous biochar derived from the pyrolysis of Mantis shrimp shell for supercapacitor electrodes. *Energy Fuel.* 35, 1557–1566. doi:10.1021/acs.energyfuels.0c04042

Huang, Y., Wu, D., Cao, D., and Cheng, D. (2018). Facile preparation of biomass-derived bifunctional electrocatalysts for oxygen reduction and evolution reactions. *Int. J. Hydrogen Energy* 43, 8611–8622. doi:10.1016/j.ijhydene.2018.03.136

IPCC (2022). "Climate change 2022: Impacts, adaptation and vulnerability." IPCC Sixth Assessment Report

Januszewicz, K., Cymann-Sachajdak, A., Kazimierski, P., Klein, M., Łuczak, J., and Wilamowska-Zawłocka, M. (2020). Chestnut-derived activated carbon as a prospective material for energy storage. *Materials* 13, 4658. doi:10.3390/ma13204658

Jia, H., Wang, S., Sun, J., Yin, K., Xie, X., and Sun, L. (2019). Nitrogen-doped microporous carbon derived from a biomass waste-metasequoia cone for electrochemical capacitors. *J. Alloy. Compd.* 794, 163–170. doi:10.1016/j.jallcom.2019.04.237

Jiang, B., Cao, L., Yuan, Q., Ma, Z., Huang, Z., Lin, Z., et al. (2022). Biomass straw-derived porous carbon synthesized for supercapacitor by ball milling. *Materials* 15, 924. doi:10.3390/ma15030924

Jiang, D., Li, H., Cheng, X., Wang, S., Abomohra, A., and Cao, B. (2022). Activation of nitrogen-doped carbon materials on the C–N bond and C–O bond: Modeling study toward enhanced pyrolysis products. *ACS Sustain. Chem. Eng.* 10, 7473–7484. doi:10.1021/acssuschemeng.1c08704

Jiang, Z., Zou, Y., Li, Y., Kong, F., and Yang, D. (2021). Environmental life cycle assessment of supercapacitor electrode production using algae derived biochar aerogel. *Biochar* 3, 701–714. doi:10.1007/s42773-021-00122-1

Jiao, S., Zhang, L., Li, C., Zhang, H., Zhang, J., Li, P., et al. (2022). Efficient construction of a carbon-based symmetric supercapacitor from soybean straw by coupling multi-stage carbonization and mild activation. *Ind. Crop. Prod.* 183, 114906. doi:10.1016/j.indcrop.2022.114906

Kasturi, P. R., Ramasamy, H., Meyrick, D., Sung Lee, Y., and Kalai Selvan, R. (2019). Preparation of starch-based porous carbon electrode and biopolymer electrolyte for all solid-state electric double layer capacitor. *J. Colloid Interf. Sci.* 554, 142–156. doi:10.1016/j.jcis.2019.06.081

Lang, J., Matějová, L., Cuentas-Gallegos, A. K., Lobato-Peralta, D. R., Ainassaari, K., Gómez, M. M., et al. (2021). Evaluation and selection of biochars and hydrochars derived from agricultural wastes for the use as adsorbent and energy storage materials. *J. Environ. Chem. Eng.* 9, 105979. doi:10.1016/j.jece.2021.105979

Lei, W., Yang, B., Sun, Y., Xiao, L., Tang, D., Chen, K., et al. (2021). Self-sacrificial template synthesis of heteroatom doped porous biochar for enhanced electrochemical energy storage. *J. Power Sources* 488, 229455. doi:10.1016/j.jpowsour.2021.229455

Leng, L., Xu, S., Liu, R., Yu, T., Zhuo, X., Leng, S., et al. (2020). Nitrogen containing functional groups of biochar: An overview. *Bioresour. Technol.* 298, 122286. doi:10.1016/j.biortech.2019.122286

Li, D., Guo, Y., Li, Y., Liu, Z., and Chen, Z. (2022). Waste-biomass tar functionalized carbon spheres with N/P Co-doping and hierarchical pores as sustainable low-cost energy storage materials. *Renew. Energy* 188, 61–69. doi:10.1016/j.renene.2022.01.109

Li, Q., Chen, D., Hu, R., Qi, J., Sui, Y., He, Y., et al. (2020). Formation of hierarchical 3D cross-linked porous carbon with small addition of graphene for supercapacitors. *Int. J. Hydrogen Energy* 45, 27471–27481. doi:10.1016/j.ijhydene.2020.07.016

Li, Q., Mu, J., Zhou, J., Zhao, Y., and Zhuo, S. (2019). Avoiding the use of corrosive activator to produce nitrogen-doped hierarchical porous carbon materials for high-performance supercapacitor electrode. *J. Electroanal. Chem.* 832, 284–292. doi:10.1016/j.jelechem.2018.11.013

Li, Q., Wu, X., Zhao, Y., Miao, Z., Xing, L., Zhou, J., et al. (2018). Nitrogen-doped hierarchical porous carbon through one-step activation of bean curd for high-performance supercapacitor electrode. *ChemElectroChem* 5, 1606–1614. doi:10.1002/celc.201800230

Li, W., Chen, C., Wang, H., Li, P., Jiang, X., Yang, J., et al. (2022). Hierarchical porous carbon induced by inherent structure of eggplant as sustainable electrode material for high performance supercapacitor. *J. Mater. Res. Technol.* 17, 1540–1552. doi:10.1016/j.jmrt.2022.01.056

Li, X., Su, Z., Liang, P., and Zhang, J. (2021a). Construction of fungus waste-derived porous carbon as electrode materials for electrochemical supercapacitor. *Biomass Convers. Biorefinery* doi:10.1007/s13399-021-01612-9

Li, X., Zhang, J., Liu, B., and Su, Z. (2021b). A critical review on the application and recent developments of post-modified biochar in supercapacitors. *J. Clean. Prod.* 310, 127428. doi:10.1016/j.jclepro.2021.127428

Li, Z., Guo, D., Liu, Y., Wang, H., and Wang, L. (2020). Recent advances and challenges in biomass-derived porous carbon nanomaterials for supercapacitors. *Chem. Eng. J.* 397, 125418. doi:10.1016/j.cej.2020.125418

Lian, J., Cheng, R., Xiong, L., Pang, D., Tian, X., Lei, J., et al. (2019a). Supercapacitors with high nitrogen content by cage-like Ganoderma lucidum spore. *Appl. Surf. Sci.* 494, 230–238. doi:10.1016/j.apsusc.2019.07.109

Lian, J., Xiong, L., Cheng, R., Pang, D., Tian, X., Lei, J., et al. (2019b). Ultra-high nitrogen content biomass carbon supercapacitors and nitrogen forms analysis. *J. Alloy. Compd.* 809, 151664. doi:10.1016/j.jallcom.2019.151664

Liang, J., Qu, T., Kun, X., Zhang, Y., Chen, S., Cao, Y., et al. (2018a). Microwave assisted synthesis of camellia oleifera shell-derived porous carbon with rich oxygen functionalities and superior supercapacitor performance. *Appl. Surf. Sci.* 436, 934–940. doi:10.1016/j.apsusc.2017.12.142

Liang, J., Tang, D., Huang, L., Chen, Y., Ren, W., and Sun, J. (2018b). High oxygen reduction reaction performance nitrogen-doped biochar cathode: A strategy for comprehensive utilizing nitrogen and carbon in water hyacinth. *Bioresour. Technol.* 267, 524–531. doi:10.1016/j.biortech.2018.07.085

Liang, X., Liu, R., and Wu, X. (2021). Biomass waste derived functionalized hierarchical porous carbon with high gravimetric and volumetric capacitances for supercapacitors. *Micropor. Mesopor. Mat.* 310, 110659. doi:10.1016/j.micromeso.2020.110659

Lima, R. M. A. P., Dos Reis, G. S., Thyrel, M., Alcaraz-Espinoza, J. J., Larsson, S. H., and de Oliveira, H. P. (2022). Facile synthesis of sustainable biomass-derived porous biochars as promising electrode materials for high-performance supercapacitor applications. *Nanomaterials* 12, 866. doi:10.3390/nano12050866

Lin, G., Ma, R., Zhou, Y., Liu, Q., Dong, X., and Wang, J. (2018). KOH activation of biomass-derived nitrogen-doped carbons for supercapacitor and electrocatalytic oxygen reduction. *Electrochim. Acta* 261, 49–57. doi:10.1016/j.electacta.2017.12.107

Liu, B., Liu, Y., Chen, H., Yang, M., and Li, H. (2017). Oxygen and nitrogen co-doped porous carbon nanosheets derived from Perilla frutescens for high volumetric performance supercapacitors. *J. Power Sources* 341, 309–317. doi:10.1016/j.jpowsour.2016.12.022

Liu, B., Yang, M., Chen, H., Liu, Y., Yang, D., and Li, H. (2018). Graphene-like porous carbon nanosheets derived from salvia splendens for high-rate performance supercapacitors. *J. Power Sources* 397, 1–10. doi:10.1016/j.jpowsour.2018.06.100

Liu, F., Ding, J., Zhao, G., Zhao, Q., Wang, K., Wang, G., et al. (2022). Catalytic pyrolysis of lotus leaves for producing nitrogen self-doping layered graphitic biochar: Performance and mechanism for peroxydisulfate activation. *Chemosphere* 302, 134868. doi:10.1016/j.chemosphere.2022.134868

Liu, H., Chen, Y., Yang, H., Hu, J., Wang, X., and Chen, H. (2022). Evolution pathway of nitrogen in hydrothermal liquefaction polygeneration of Spirulina as the typical high-protein microalgae. *Algal Res.* 66, 102759. doi:10.1016/j.algal.2022.102759

Liu, H., Liu, R., Xu, C., Ren, Y., Tang, D., Zhang, C., et al. (2020). Oxygen–nitrogen–sulfur self-doping hierarchical porous carbon derived from lotus leaves for high-performance supercapacitor electrodes. *J. Power Sources* 479, 228799. doi:10.1016/j.jpowsour.2020.228799

Liu, S., He, Z., Dong, Q., Zhao, A., Huang, F., and Bi, D. (2022). Comparative assessment of water and organic acid washing pretreatment for nitrogen-rich pyrolysis: Characteristics and distribution of bio-oil and biochar. *Biomass Bioenergy* 161, 106480. doi:10.1016/j.biombioe.2022.106480

Liu, X., Luo, Z., Yu, C., and Xie, G. (2019). Conversion mechanism of fuel-N during pyrolysis of biomass wastes. *Fuel* 246, 42–50. doi:10.1016/j.fuel.2019.02.042

Liu, Y., Dai, G., Zhu, L., and Wang, S. (2018). Green conversion of microalgae into high-performance sponge-like nitrogen-enriched carbon. *ChemElectroChem* 6, 646–652. doi:10.1002/celc.201801272

Liu, Z., Tian, D., Shen, F., Nnanna, P. C., Hu, J., Zeng, Y., et al. (2020). Valorization of composting leachate for preparing carbon material to achieve high electrochemical performances for supercapacitor electrode. *J. Power Sources* 458, 228057. doi:10.1016/j.jpowsour.2020.228057

Liu, Z., Zhang, Y., and Liu, Z. (2019). Comparative production of biochars from corn stalk and cow manure. *Bioresour. Technol.* 291, 121855. doi:10.1016/j.biortech.2019.121855

Luo, M., Zhu, Z., Yang, K., Yang, P., Miao, Y., Chen, M., et al. (2020). Sustainable biomass-based hierarchical porous carbon for energy storage: A novel route to maintain electrochemically attractive natural structure of precursor. *Sci. Total Environ.* 747, 141923. doi:10.1016/j.scitotenv.2020.141923

Ma, G., Zhang, Z., Peng, H., Sun, K., Ran, F., and Lei, Z. (2016). Facile preparation of nitrogen-doped porous carbon for high performance symmetric supercapacitor. *J. Solid State Electr.* 20, 1613–1623. doi:10.1007/s10008-016-3171-1

Ma, H., Li, C., Zhang, M., Hong, J., and Shi, G. (2017). Graphene oxide induced hydrothermal carbonization of egg proteins for high-performance supercapacitors. *J. Mat. Chem. A* 5, 17040–17047. doi:10.1039/C7TA04771A

Ma, Y., Yin, J., Liang, H., Yao, D., Xia, Y., Zuo, K., et al. (2021). A two step approach for making super capacitors from waste wood. *J. Clean. Prod.* 279, 123786. doi:10.1016/j.jclepro.2020.123786

Ma, Z., Zhang, Z., Qu, Y., Lai, F., Li, Q., Wu, X., et al. (2019). Yeast protein derived hierarchical mesoporous carbon for symmetrical capacitor with excellent electrochemical performances. *Micropor. Mesopor. Mat.* 281, 50–56. doi:10.1016/j.micromeso.2019.02.013

MacDermid-Watts, K., Pradhan, R., and Dutta, A. (2020). Catalytic hydrothermal carbonization treatment of biomass for enhanced activated carbon: A review. *Waste biomass valorization* 12, 2171. doi:10.1007/s12649-020-01134-x

Martínez-Casillas, D. C., Alonso-Lemus, I. L., Mascorro-Gutiérrez, I., and Cuentas-Gallegos, A. K. (2018). Leather waste-derived biochar with high performance for supercapacitors. *J. Electrochem. Soc.* 165, A2061–A2068. doi:10.1149/2.0421810jes

Mehdi, R., Khoja, A. H., Naqvi, S. R., Gao, N., and Amin, N. A. S. (2022). A review on production and surface modifications of biochar materials via biomass pyrolysis process for supercapacitor applications. *Catalysts* 12, 798. doi:10.3390/catal12070798

Meyer, S., Glaser, B., and Quicker, P. (2011). Technical, economical, and climate-related aspects of biochar production technologies: A literature review. *Environ. Sci. Technol.* 45, 9473–9483. doi:10.1021/es201792c

Mondal, A. K., Kretschmer, K., Zhao, Y., Liu, H., Fan, H., and Wang, G. (2017a). Naturally nitrogen doped porous carbon derived from waste shrimp shells for high-performance lithium ion batteries and supercapacitors. *Micropor. Mesopor. Mat.* 246, 72–80. doi:10.1016/j.micromeso.2017.03.019

Mondal, A. K., Kretschmer, K., Zhao, Y., Liu, H., Wang, C., Sun, B., et al. (2017b). Nitrogen-doped porous carbon nanosheets from eco-friendly Eucalyptus leaves as high performance electrode materials for supercapacitors and lithium ion batteries. *Chem. - A Eur. J.* 23, 3683–3690. doi:10.1002/chem.201605019

Niu, B., Yuan, M., Jiang, F., and Li, M. (2019b). Protein powder derived porous carbon materials as supercapacitor electrodes. *Int. J. Electrochem. Sc.* 2019, 3253–3264. doi:10.20964/2019.04.33

Niu, J., Liu, M., Xu, F., Zhang, Z., Dou, M., and Wang, F. (2018). Synchronously boosting gravimetric and volumetric performance: Biomass-derived ternary-doped microporous carbon nanosheet electrodes for supercapacitors. *Carbon* 140, 664–672. doi:10.1016/j.carbon.2018.08.036

Niu, L., Shen, C., Yan, L., Zhang, J., Lin, Y., Gong, Y., et al. (2019a). Waste bones derived nitrogen–doped carbon with high micropore ratio towards supercapacitor applications. *J. Colloid Interf. Sci.* 547, 92–101. doi:10.1016/j.jcis.2019.03.097

Norouzi, O., Pourhosseini, S. E. M., Naderi, H. R., Di Maria, F., and Dutta, A. (2021). Integrated hybrid architecture of metal and biochar for high performance asymmetric supercapacitors. *Sci. Rep.-UK* 11, 5387. doi:10.1038/s41598-021-84979-z

Parsimehr, H., Ehsani, A., and Payam, S. A. (2022). Electrochemical energy storage electrodes from rice biochar. *Biomass Convers. Biorefinery*. doi:10.1007/s13399-021-02089-2

Perez-Salcedo, K. Y., Ruan, S., Su, J., Shi, X., Kannan, A. M., and Escobar, B. (2020). Seaweed-derived KOH activated biocarbon for electrocatalytic oxygen reduction and supercapacitor applications. *J. Porous Mat.* 27, 959–969. doi:10.1007/s10934-020-00871-7

Qi, J., Zhang, W., and Xu, L. (2018). Solvent-free mechanochemical preparation of hierarchically porous carbon for supercapacitor and oxygen reduction reaction. *Chem. – A Eur. J.* 24, 18097–18105. doi:10.1002/chem.201804302

Qin, L., Wu, Y., and Jiang, E. (2022). *In situ* template preparation of porous carbon materials that are derived from swine manure and have ordered hierarchical nanopore structures for energy storage. *Energy* 242, 123040. doi:10.1016/j.energy.2021.123040

Raj, C. J., Rajesh, M., Manikandan, R., Yu, K. H., Anusha, J. R., Ahn, J. H., et al. (2018). High electrochemical capacitor performance of oxygen and nitrogen enriched activated carbon derived from the pyrolysis and activation of squid gladius chitin. *J. Power Sources* 386, 66–76. doi:10.1016/j.jpowsour.2018.03.038

Rawat, S., Mishra, R. K., and Bhaskar, T. (2022). Biomass derived functional carbon materials for supercapacitor applications. *Chemosphere* 286, 131961. doi:10.1016/j.chemosphere.2021.131961

Ren, M., Jia, Z., Tian, Z., Lopez, D., Cai, J., Titirici, M. M., et al. (2018). High performance N-doped carbon electrodes obtained via hydrothermal carbonization of macroalgae for supercapacitor applications. *ChemElectroChem* 5, 2686–2693. doi:10.1002/celc.201800603

Rong, X., Xie, M., Kong, L., Natarajan, V., Ma, L., and Zhan, J. (2019). The magnetic biochar derived from banana peels as a persulfate activator for organic contaminants degradation. *Chem. Eng. J.* 372, 294–303. doi:10.1016/j.cej.2019.04.135

Sangprasert, T., Sattayarut, V., Rajrujithong, C., Khanchaitit, P., Khemthong, P., Chanthad, C., et al. (2022). Making use of the inherent nitrogen content of spent coffee grounds to create nanostructured activated carbon for supercapacitor and lithium-ion battery applications. *Diam. Relat. Mat.* 127, 109164. doi:10.1016/j.diamond.2022.109164

Sankaranarayanan, S., Hariram, M., Vivekanandhan, S., and Navia, R. (2021). Sustainable biocarbon materials derived from Lessonia Trabeculata macroalgae biomass residue for supercapacitor applications. *Energy storage* 3, n/a. doi:10.1002/est2.222

Sattayarut, V., Wanchaem, T., Ukkakimapan, P., Yordsri, V., Dulyaseree, P., Phonyiem, M., et al. (2019). Nitrogen self-doped activated carbonsvia the direct activation ofSamanea saman leaves for high energy density supercapacitors. *RSC Adv.* 9, 21724–21732. doi:10.1039/C9RA03437D

Shao, R., Niu, J., Liang, J., Liu, M., Zhang, Z., Dou, M., et al. (2017). Mesopore- and macropore-dominant nitrogen-doped hierarchically porous carbons for high-energy and ultrafast supercapacitors in non-aqueous electrolytes. *ACS Appl. Mater Interfaces* 9, 42797–42805. doi:10.1021/acsami.7b14390

Shen, F., Zhu, L., and Qi, X. (2018). Nitrogen self-doped hierarchical porous carbon from Myriophyllum aquaticum for supercapacitor electrode. *ChemistrySelect* 3, 11350–11356. doi:10.1002/slct.201802400

Shi, Y., Zhang, L., Schon, T. B., Li, H., Fan, C., Li, X., et al. (2017). Porous carbon with willow-leaf-shaped pores for high-performance supercapacitors. *ACS Appl. Mat. Inter.* 9, 42699–42707. doi:10.1021/acsami.7b12776

Si, W., Zhou, J., Zhang, S., Li, S., Xing, W., and Zhuo, S. (2013). Tunable N-doped or dual N, S-doped activated hydrothermal carbons derived from human hair and glucose for supercapacitor applications. *Electrochim. Acta* 107, 397–405. doi:10.1016/j.electacta.2013.06.065

Sinha, P., Yadav, A., Tyagi, A., Paik, P., Yokoi, H., Naskar, A. K., et al. (2020). Keratin-derived functional carbon with superior charge storage and transport for high-performance supercapacitors. *Carbon* 168, 419–438. doi:10.1016/j.carbon.2020.07.007

Song, M., Zhou, Y., Ren, X., Wan, J., Du, Y., Wu, G., et al. (2019). Biowaste-based porous carbon for supercapacitor: The influence of preparation processes on structure and performance. *J. Colloid Interf. Sci.* 535, 276–286. doi:10.1016/j.jcis.2018.09.055

Song, P., Shen, X., He, W., Kong, L., He, X., Ji, Z., et al. (2018). Protein-derived nitrogen-doped hierarchically porous carbon as electrode material for supercapacitors. *J. Mater. Sci. Mater. Electron.* 29, 12206–12215. doi:10.1007/s10854-018-9329-0

Soroush, S., Ronsse, F., Verberckmoes, A., Verpoort, F., Park, J., Wu, D., et al. (2022). Production of solid hydrochar from waste seaweed by hydrothermal carbonization: Effect of process variables. *Biomass Convers. Biorefinery* doi:10.1007/s13399-022-02365-9

Stobernack, N., Mayer, F., Malek, C., and Bhandari, R. (2020). Evaluation of the energetic and environmental potential of the hydrothermal carbonization of biowaste: Modeling of the entire process chain. *Bioresour. Technol.* 318, 124038. doi:10.1016/j.biortech.2020.124038

Sun, J., Norouzi, O., and Mašek, O. (2022). A state-of-the-art review on algae pyrolysis for bioenergy and biochar production. *Bioresour. Technol.* 346, 126258. doi:10.1016/j.biortech.2021.126258

Sun, Q., Cao, Z., Wang, S., Sun, L., Zhou, L., Xue, H., et al. (2020). Bio-inspired heteroatom-doped hollow aurilave-like structured carbon for high-performance sodium-ion batteries and supercapacitors. *J. Power Sources* 461, 228128. doi:10.1016/j.jpowsour.2020.228128

Sun, Y., Xue, J., Dong, S., Zhang, Y., An, Y., Ding, B., et al. (2020). Biomass-derived porous carbon electrodes for high-performance supercapacitors. *J. Mat. Sci.* 55, 5166–5176. doi:10.1007/s10853-019-04343-5

Sun, Z. (2017). Nitrogen self-doped porous carbon materials derived from a new biomass source for highly stable supercapacitors. *Int. J. Electrochem. Sc.* 2017, 12084–12097. doi:10.20964/2017.12.400

Tang, L., Zhou, Y., Zhou, X., Chai, Y., Zheng, Q., and Lin, D. (2019). Enhancement in electrochemical performance of nitrogen-doped hierarchical porous carbon-based supercapacitor by optimizing activation temperature. *J. Mater. Sci. Mater. Electron.* 30, 2600–2609. doi:10.1007/s10854-018-0535-6

Tang, W., Zhang, Y., Zhong, Y., Shen, T., Wang, X., Xia, X., et al. (2017). Natural biomass-derived carbons for electrochemical energy storage. *Mat. Res. Bull.* 88, 234–241. doi:10.1016/j.materresbull.2016.12.025

Wahid, M., Parte, G., Phase, D., and Ogale, S. (2015). Yogurt: A novel precursor for heavily nitrogen doped supercapacitor carbon. *J. Mat. Chem. A* 3, 1208–1215. doi:10.1039/C4TA06068G

Wan, L., Song, P., Liu, J., Chen, D., Xiao, R., Zhang, Y., et al. (2019). Facile synthesis of nitrogen self-doped hierarchical porous carbon derived from pine pollen via MgCO3 activation for high-performance supercapacitors. *J. Power Sources* 438, 227013. doi:10.1016/j.jpowsour.2019.227013

Wang, C., Wang, H., Yang, C., Dang, B., Li, C., and Sun, Q. (2020). A multilevel gradient structural carbon derived from naturally preprocessed biomass. *Carbon* 168, 624–632. doi:10.1016/j.carbon.2020.07.020

Wang, C., Wu, D., Wang, H., Gao, Z., Xu, F., and Jiang, K. (2018). Biomass derived nitrogen-doped hierarchical porous carbon sheets for supercapacitors with high performance. *J. Colloid Interf. Sci.* 523, 133–143. doi:10.1016/j.jcis.2018.03.009

Wang, C., Wu, D., Wang, H., Gao, Z., Xu, F., and Jiang, K. (2017). Nitrogen-doped two-dimensional porous carbon sheets derived from clover biomass for high performance supercapacitors. *J. Power Sources* 363, 375–383. doi:10.1016/j.jpowsour.2017.07.097

Wang, D., Li, F., Yin, L., Lu, X., Chen, Z., Gentle, I. R., et al. (2012). Nitrogen-doped carbon monolith for alkaline supercapacitors and understanding nitrogen-induced redox transitions. *Chem. - A Eur. J.* 18, 5345–5351. doi:10.1002/chem.201102806

Wang, D., Xu, Z., Lian, Y., Ban, C., and Zhang, H. (2019). Nitrogen self-doped porous carbon with layered structure derived from porcine bladders for high-performance supercapacitors. *J. Colloid Interf. Sci.* 542, 400–409. doi:10.1016/j.jcis.2019.02.024

Wang, J., Li, Z., Yan, S., Yu, X., Ma, Y., and Ma, L. (2019). Modifying the microstructure of algae-based active carbon and modelling supercapacitors using artificial neural networks. *RSC Adv.* 9, 14797–14808. doi:10.1039/C9RA01255A

Wang, J., and Liu, Q. (2015). Fungi-derived hierarchically porous carbons for high-performance supercapacitors. *RSC Adv.* 5, 4396–4403. doi:10.1039/C4RA13358G

Wang, J., Ma, C., Su, L., Gong, L., Dong, D., and Wu, Z. (2020). Self-assembly/Sacrificial synthesis of highly capacitive hierarchical porous carbon from longan pulp biomass. *ChemElectroChem* 7, 4606–4613. doi:10.1002/celc.202001129

Wang, J., Wan, F., Lü, Q., Chen, F., and Lin, Q. (2018). Self-nitrogen-doped porous biochar derived from kapok (Ceiba insignis) fibers: Effect of pyrolysis temperature and high electrochemical performance. *J. Mat. Sci. Technol.* 34, 1959–1968. doi:10.1016/j.jmst.2018.01.005

Wang, K., Zhao, N., Lei, S., Yan, R., Tian, X., Wang, J., et al. (2015). Promising biomass-based activated carbons derived from willow catkins for high performance supercapacitors. *Electrochim. Acta* 166, 1–11. doi:10.1016/j.electacta.2015.03.048

Wang, Q., Xiong, J., Song, Q., Shaheen, S. M., Salem, H. M. S., Mohamed, I., et al. (2022). Preparation of nitrogen-enriched Fe-doped porous biochar using the catalytic pyrolysis of paper mill sludge. *Biomass Convers. Biorefinery* 2022. doi:10.1007/s13399-022-03209-2

Wang, S., Shi, Y., Xiang, H., Liu, R., Su, L., Zhang, L., et al. (2022). Functional utilization of biochar derived fromTenebrio molitor feces for CO2 capture and supercapacitor applications. *RSC Adv.* 12, 22760–22769. doi:10.1039/D2RA03575H

Wang, X., Jiang, T., Nasser, R., Cao, Q., Gong, M., Li, X., et al. (2022). Preparation of *in-situ* N/O co-doped lily-derived porous carbon framework material and its application in supercapacitors. *Biomass Bioenergy* 166, 106602. doi:10.1016/j.biombioe.2022.106602

Wang, Y., Jiang, H., Ye, S., Zhou, J., Chen, J., and Zeng, Q. (2018). N-doped porous carbon derived from walnut shells with enhanced electrochemical performance for supercapacitor. *Funct. Mater. Lett.* 12, 1950042. doi:10.1142/S1793604719500425

Wang, Y., Zhang, M., Dai, Y., Wang, H., Zhang, H., Wang, Q., et al. (2019). Nitrogen and phosphorus co-doped silkworm-cocoon-based self-activated porous carbon for high performance supercapacitors. *J. Power Sources* 438, 227045. doi:10.1016/j.jpowsour.2019.227045

Wei, T., Wei, X., Gao, Y., and Li, H. (2015). Large scale production of biomass-derived nitrogen-doped porous carbon materials for supercapacitors. *Electrochim. Acta* 169, 186–194. doi:10.1016/j.electacta.2015.04.082

Wen, X., Lu, X., Xiang, K., Xiao, L., Liao, H., Chen, W., et al. (2019). Nitrogen/sulfur co-doped ordered carbon nanoarrays for superior sulfur hosts in lithium-sulfur batteries. *J. Colloid Interf. Sci.* 554, 711–721. doi:10.1016/j.jcis.2019.07.057

Wesley, R. J., Durairaj, A., Ramanathan, S., Abraham, R. J., Obadiah, A., Ramasundaram, S., et al. (2022). Tea waste biochar composite with nickel phthalocyanine as a potential supercapacitor electrode material. *Biomass Convers. Biorefinery* 2022. doi:10.1007/s13399-021-02206-1

Xia, C., Surendran, S., Ji, S., Kim, D., Chae, Y., Kim, J., et al. (2022). A sulfur self-doped multifunctional biochar catalyst for overall water splitting and a supercapacitor from Camellia japonica flowers. *Carbon Energy* 4, 491–505. doi:10.1002/cey2.207

Xie, Q., Qu, S., Zhao, Y., Zhang, Y., and Zhao, P. (2019). N/O co-enriched amorphous carbon coated graphene with a sandwiched porous architecture as supercapacitor electrodes with high volumetric specific capacitance. *J. Mater. Sci. Mater. Electron.* 30, 20265–20275. doi:10.1007/s10854-019-02411-9

Xu, B., Hou, S., Zhang, F., Cao, G., Chu, M., and Yang, Y. (2014). Nitrogen-doped mesoporous carbon derived from biopolymer as electrode material for supercapacitors. *J. Electroanal. Chem.* 712, 146–150. doi:10.1016/j.jelechem.2013.11.020

Xu, G., Han, J., Ding, B., Nie, P., Pan, J., Dou, H., et al. (2015). Biomass-derived porous carbon materials with sulfur and nitrogen dual-doping for energy storage. *Green Chem.* 17, 1668–1674. doi:10.1039/C4GC02185A

Xu, S., Chen, J., Peng, H., Leng, S., Li, H., Qu, W., et al. (2021). Effect of biomass type and pyrolysis temperature on nitrogen in biochar, and the comparison with hydrochar. *Fuel* 291, 120128. doi:10.1016/j.fuel.2021.120128

Xu, S., Zhao, Y., Xu, Y., Chen, Q., Zhang, G., Xu, Q., et al. (2018). Heteroatom doped porous carbon sheets derived from protein-rich wheat gluten for supercapacitors: The synergistic effect of pore properties and heteroatom on the electrochemical performance in different electrolytes. *J. Power Sources* 401, 375–385. doi:10.1016/j.jpowsour.2018.09.012

Xu, Z., Li, Y., Li, D., Wang, D., Zhao, J., Wang, Z., et al. (2018). N-enriched multilayered porous carbon derived from natural casings for high-performance supercapacitors. *Appl. Surf. Sci.* 444, 661–671. doi:10.1016/j.apsusc.2018.03.100

Xue, C., Wei, Y., Huang, R., Zhao, W., Wu, T., Li, X., et al. (2022). Magnesium oxide scaffolded preparation of N, O self-doped biochar with super-hydrophilic surface for aqueous supercapacitor with desired energy density. *J. Energy Storage* 53, 105193. doi:10.1016/j.est.2022.105193

Yan, J., Wang, Q., Wei, T., and Fan, Z. (2014). Recent advances in design and fabrication of electrochemical supercapacitors with high energy densities. *Adv. Energy Mat.* 4, 1300816. doi:10.1002/aenm.201300816

Yan, J. (2020). Nitrogen-doped oxygen-rich activated carbon derived from longan shell for supercapacitors. *Int. J. Electrochem. Sc.* 2020, 1982–1995. doi:10.20964/2020.03.18

Yan, W., Meng, Z., Zou, M., Miao, H., Ma, F., Yu, R., et al. (2020). Neutralization reaction in synthesis of carbon materials for supercapacitors. *Chem. Eng. J.* 381, 122547. doi:10.1016/j.cej.2019.122547

Yang, J., Wang, Y., Luo, J., and Chen, L. (2018). Highly nitrogen-doped graphitic carbon fibers from sustainable plant protein for supercapacitor. *Ind. Crop. Prod.* 121, 226–235. doi:10.1016/j.indcrop.2018.05.013

Yang, J., Yang, H., Wang, S., Wang, K., Sun, Y., Yi, W., et al. (2023). Importance of pyrolysis programs in enhancing the application of microalgae-derived biochar in microbial fuel cells. *Fuel* 333, 126244. doi:10.1016/j.fuel.2022.126244

Yao, S., Zhang, Z., Wang, Y., Liu, Z., and Li, Z. (2021). Simple one-pot strategy for converting biowaste into valuable graphitized hierarchically porous biochar for high-efficiency capacitive storage. *J. Energy Storage* 44, 103259. doi:10.1016/j.est.2021.103259

Yu, J., Li, X., Cui, Z., Chen, D., Pang, X., Zhang, Q., et al. (2021). Tailoring *in-situ* N, O, P, S-doped soybean-derived porous carbon with ultrahigh capacitance in both acidic and alkaline media. *Renew. Energy* 163, 375–385. doi:10.1016/j.renene.2020.08.066

Yu, J., Tang, L., Pang, Y., Zeng, G., Wang, J., Deng, Y., et al. (2019). Magnetic nitrogen-doped sludge-derived biochar catalysts for persulfate activation: Internal electron transfer mechanism. *Chem. Eng. J.* 364, 146–159. doi:10.1016/j.cej.2019.01.163

Yu, W., Wang, H., Liu, S., Mao, N., Liu, X., Shi, J., et al. (2016). N, O-codoped hierarchical porous carbons derived from algae for high-capacity supercapacitors and battery anodes. *J. Mat. Chem. A* 4, 5973–5983. doi:10.1039/C6TA01821A

Yuan, C., Chen, M., Zhu, K., Ni, J., Wang, S., Cao, B., et al. (2022). Facile synthesis of nitrogen-doped interconnected porous carbons derived from reed and chlorella for high-performance supercapacitors. *Fuel Process Technol.* 238, 107466. doi:10.1016/j.fuproc.2022.107466

Yuan, G., Guan, K., Hu, H., Lei, B., Xiao, Y., Dong, H., et al. (2021). Calcium-chloride-assisted approach towards green and sustainable synthesis of hierarchical porous carbon microspheres for high-performance supercapacitive energy storage. *J. Colloid Interf. Sci.* 582, 159–166. doi:10.1016/j.jcis.2020.07.082

Yuan, X., Dissanayake, P. D., Gao, B., Liu, W., Lee, K. B., and Ok, Y. S. (2021). Review on upgrading organic waste to value-added carbon materials for energy and environmental applications. *J. Environ. Manage.* 296, 113128. doi:10.1016/j.jenvman.2021.113128

Yuan, X., Xiao, J., Yılmaz, M., Zhang, T. C., and Yuan, S. (2022). N, P Co-doped porous biochar derived from cornstalk for high performance CO2 adsorption and electrochemical energy storage. *Sep. Purif. Technol.* 299, 121719. doi:10.1016/j.seppur.2022.121719

Zhan, H., Zhuang, X., Song, Y., Yin, X., and Wu, C. (2018). Insights into the evolution of fuel-N to NO precursors during pyrolysis of N-rich nonlignocellulosic biomass. *Appl. Energy* 219, 20–33. doi:10.1016/j.apenergy.2018.03.015

Zhang, L., Song, X., Xiao, B., Tan, L., Ma, H., Wang, X., et al. (2019). Highly graphitized and N, O co-doped porous carbon derived from leaves of viburnum sargenti with outstanding electrochemical performance for effective supercapacitors. *Colloids Surfaces A Physicochem. Eng. Aspects* 580, 123721. doi:10.1016/j.colsurfa.2019.123721

Zhang, P., Li, Y., Cao, Y., and Han, L. (2019). Characteristics of tetracycline adsorption by cow manure biochar prepared at different pyrolysis temperatures. *Bioresour. Technol.* 285, 121348. doi:10.1016/j.biortech.2019.121348

Zhang, W., Tian, H., Cheng, R., Wang, Z., Ma, Y., Ran, S., et al. (2020). A composite-hydroxide-activation strategy for the preparation of N/S dual-doped porous carbon materials as advanced supercapacitor electrodes. *J. Mater. Sci. Mater. Electron.* 31, 22498–22511. doi:10.1007/s10854-020-04751-3

Zhang, X., Cai, W., Zhao, S., Li, X., Jia, F., Ma, F., et al. (2021). Discarded antibiotic mycelial residues derived nitrogen-doped porous carbon for electrochemical energy storage and simultaneous reduction of antibiotic resistance genes(ARGs). *Environ. Res.* 192, 110261. doi:10.1016/j.envres.2020.110261

Zhang, X., Ma, X., Yu, Z., Yi, Y., Huang, Z., and Lu, C. (2022). Preparation of high-value porous carbon by microwave treatment of chili straw pyrolysis residue. *Bioresour. Technol.* 360, 127520. doi:10.1016/j.biortech.2022.127520

Zhao, G., Yu, D., Chen, C., Sun, L., Yang, C., Zhang, H., et al. (2020). One-step production of carbon nanocages for supercapacitors and sodium-ion batteries. *J. Electroanal. Chem.* 878, 114551. doi:10.1016/j.jelechem.2020.114551

Zhao, Y., Lu, M., Tao, P., Zhang, Y., Gong, X., Yang, Z., et al. (2016). Hierarchically porous and heteroatom doped carbon derived from tobacco rods for supercapacitors. *J. Power Sources* 307, 391–400. doi:10.1016/j.jpowsour.2016.01.020

Zhou, J., Yuan, S., Lu, C., Yang, M., and Song, Y. (2020). Hierarchical porous carbon microtubes derived from corn silks for supercapacitors electrode materials. *J. Electroanal. Chem.* 878, 114704. doi:10.1016/j.jelechem.2020.114704

Zhou, N., Zu, J., Xu, F., Wang, Y., Luo, Y., Li, S., et al. (2020). The preparation of N, S, P self-doped and oxygen functionalized porous carbon via aerophilic interface reaction for high-performance supercapacitors. *J. Mater. Sci. Mater. Electron.* 31, 12961–12972. doi:10.1007/s10854-020-03849-y

Zhou, R., Wang, X., Zhou, R., Weerasinghe, J., Zhang, T., Xin, Y., et al. (2022). Non-thermal plasma enhances performances of biochar in wastewater treatment and energy storage applications. *Front. Chem. Sci. Eng.* 16, 475–483. doi:10.1007/s11705-021-2070-x

Zhou, Y., Qin, S., Verma, S., Sar, T., Sarsaiya, S., Ravindran, B., et al. (2021). Production and beneficial impact of biochar for environmental application: A comprehensive review. *Bioresour. Technol.* 337, 125451. doi:10.1016/j.biortech.2021.125451

Zhou, Y., Ren, J., Xia, L., Zheng, Q., Liao, J., Long, E., et al. (2018). Waste soybean dreg-derived N/O co-doped hierarchical porous carbon for high performance supercapacitor. *Electrochim. Acta* 284, 336–345. doi:10.1016/j.electacta.2018.07.134

Zhu, B., Liu, B., Qu, C., Zhang, H., Guo, W., Liang, Z., et al. (2018). Tailoring biomass-derived carbon for high-performance supercapacitors from controllably cultivated algae microspheres. *J. Mat. Chem. A* 6, 1523–1530. doi:10.1039/C7TA09608A

Zhu, H., Yin, J., Wang, X., Wang, H., and Yang, X. (2013). Microorganism-derived heteroatom-doped carbon materials for oxygen reduction and supercapacitors. *Adv. Funct. Mat.* 23, 1305–1312. doi:10.1002/adfm.201201643

Zhu, L., Shen, F., Smith, R. L., and Qi, X. (2017). High-performance supercapacitor electrode materials from chitosan via hydrothermal carbonization and potassium hydroxide activation. *Energy Technol.* 5, 452–460. doi:10.1002/ente.201600337

Zhu, X., Yang, S., Wang, L., Liu, Y., Qian, F., Yao, W., et al. (2016). Tracking the conversion of nitrogen during pyrolysis of antibiotic mycelial fermentation residues using XPS and TG-FTIR-MS technology. *Environ. Pollut.* 211, 20–27. doi:10.1016/j.envpol.2015.12.032

Zhu, Y., Fang, T., Hua, J., Qiu, S., Chu, H., Zou, Y., et al. (2019). Biomass-derived porous carbon prepared from egg white for high-performance supercapacitor electrode materials. *ChemistrySelect* 4, 7358–7365. doi:10.1002/slct.201901632

Zhu, Z., and Xu, Z. (2020). The rational design of biomass-derived carbon materials towards next-generation energy storage: A review. *Renew. Sustain. Energy Rev.* 134, 110308. doi:10.1016/j.rser.2020.110308

Zou, Z., Lei, Y., Li, Y., Zhang, Y., and Xiao, W. (2019). Nitrogen-doped hierarchical meso/microporous carbon from bamboo fungus for symmetric supercapacitor applications. *Molecules* 24, 3677. doi:10.3390/molecules24203677